

## Tricritical coexistence in three dimensions: The multicomponent limit

Stéphane Sarbach

*Baker Laboratory, Cornell University, Ithaca, New York 14853  
and Institut für Festkörperforschung, Kernforschungsanlage Jülich,  
Postfach 1913, D-5170 Jülich, West Germany*

Michael E. Fisher

*Baker Laboratory, Cornell University, Ithaca, New York 14853  
(Received 7 May 1979)*

The asymptotic tricritical equation of state, including the three-phase coexistence monohedron, is analyzed in detail for the exactly soluble multicomponent or spherical limit,  $n \rightarrow \infty$ , of the continuous-spin model with terms of order  $s^3$ ,  $s^4$ , and  $s^6$ , in  $d=3$  spatial dimensions. Various nonuniversal scaling functions and amplitude ratios, depending on the range parameter  $z \propto 1/R_0^3$ , are evaluated explicitly and reveal the nature and magnitude of the deviations from the classical, phenomenological theory of tricriticality (which is developed systematically in an Appendix). The relationship to results for finite  $n$  is discussed briefly.

### I. INTRODUCTION

Our understanding of the equation of state of a real, three-dimensional physical system in the vicinity of a tricritical point is, despite significant theoretical<sup>1-3</sup> and experimental<sup>4-6</sup> progress, still seriously incomplete. Theoretically,  $d=3$  dimensions represents a particularly interesting case as, on the basis of renormalization-group arguments,<sup>1</sup> it is expected to be the borderline dimension for tricriticality, above which the tricritical exponents should take on their classical or phenomenological,<sup>2</sup>  $d$ -independent values. At a border-line dimension the appearance of a marginal operator or physical density is anticipated,<sup>1,3</sup> and such marginal operators generally lead to logarithmic correction factors to classical power-law behavior.<sup>1,3</sup> Furthermore, marginality may be associated with nonuniversal features.

Current experiments<sup>4-7</sup> agree well with the theoretical expectations in that the observed tricritical exponents are quite consistent with the classical values. On the other hand, the predicted logarithmic correction factors,<sup>3</sup> have not been observed, even in the most careful experiments [see, e.g., Ref. 5(c)]. However, as recently stressed,<sup>7</sup> the experimental data do exhibit unambiguous deviations from other predictions of the phenomenological theory of the tricritical equation of state.

We have recently demonstrated<sup>7</sup> that the multicomponent,  $n \rightarrow \infty$ , or spherical model limit enables one to study in exact analytical terms<sup>8-10</sup> the deviations from classical theory. In that limit no logarithmic corrections to power-law behavior are found; however, it was shown that, although the tricritical exponents are classical, the equation of state deviates significantly, and in a *nonuniversal* way, from the clas-

sical predictions. Furthermore, the nonuniversality is parametrized by a *single* (marginal) variable,  $p$  or  $z$ , related to the finite range of the basic pair interactions. This parameter vanishes for infinite-ranged (infinitely weak) forces; the theory then reproduces the classical results, as expected in this, so-called, van der Waals limit. Because the nonuniversality is governed by only one parameter, there are definite relations, which can be displayed explicitly,<sup>7</sup> between any pair of dimensionless amplitude ratios characterizing the asymptotic tricritical behavior. Despite the fact that real physical systems, such as <sup>3</sup>He-<sup>4</sup>He mixtures,<sup>4</sup> metamagnets,<sup>5</sup> and multicomponent fluid mixtures,<sup>6</sup> should be described by models with order parameters having only  $n=1$  or 2 components, the amplitude-ratio relations found for  $n \rightarrow \infty$  correlate surprisingly well with experimental observations.<sup>7</sup> Among the most interesting amplitude ratios are those describing the coexistence of various phases below a tricritical point: these can be studied by introducing a "cubic" or "third-order" field,  $h_3$ , which can also be accomplished analytically<sup>8</sup> in the  $n \rightarrow \infty$  limit.

The main goal of the present paper is to present the derivation of the detailed results for the tricritical equation of state in the multicomponent limit, in particular the various important amplitude-ratio relations, which were announced in Ref. 7. The analysis, which unfortunately is rather heavy algebraically, relies on the general solution for the  $n \rightarrow \infty$  limit given in Ref. 8 (which will hereafter be referred to as I). The principal results from Ref. 8 are recalled in Sec. II below. In Sec. III the asymptotic tricritical behavior is studied in the symmetry plane in which the two relevant odd fields,  $h$  and  $h_3$ , both vanish. The general tricritical neighborhood (with  $h$  and  $h_3$

nonzero) is taken up in Sec. IV, where the nonclassical effects on the shape of the three-phase monohedron<sup>7</sup> are elucidated.

The classical phenomenological theory of the tricritical equation of state is developed in detail in the Appendix: this material is not completely new or original, but the analysis is somewhat tricky and no explicit derivations seem to be in the literature. Furthermore, the results are needed as a leading approximation in studying the  $n \rightarrow \infty$ , spherical model limit for small nonuniversality parameter. Finally, in Sec. V, some concluding remarks are presented, and the expected behavior for finite  $n$  is discussed in terms of a renormalized value of the range parameter  $z$ .

## II. MULTICOMPONENT LIMIT

In Ref. 8 (hereafter referred to as I) we have shown how to derive the free energy and equation of state of a  $d$ -dimensional,  $n$ -component spin model with a Hamiltonian of Landau-Ginzburg-Wilson type, in the multicomponent,  $n \rightarrow \infty$ , or, equivalently, spherical model limit. In this section we summarize the results obtained in I and present them in a form more suitable for the study of the nonuniversal tricritical behavior.

The model consists of a set of  $n$ -component, classical spins,  $\vec{s}_i = (s_i^\mu)$  with  $\mu = 1, 2, \dots, n$ , located on the sites  $i = 1, \dots, N$ , of a regular  $d$ -dimensional lattice and interacting through the Hamiltonian

$$\mathcal{H}(\{\vec{s}_j\}) = \mathcal{H}^1(\{\vec{s}_j\}) - \sum_{j=1}^N \left[ \vec{H} \cdot \vec{s}_j + \frac{(\vec{H}_3 \cdot \vec{s}_j) |\vec{s}_j|^2}{n} \right] + \sum_{j=1}^N \left[ \frac{1}{2} D |\vec{s}_j|^2 + \frac{1}{4} \frac{U |\vec{s}_j|^4}{n} + \frac{1}{6} \frac{V |\vec{s}_j|^6}{n^2} \right], \quad (2.1)$$

where

$$\vec{H} = (H, H, \dots, H), \quad \vec{H}_3 = (H_3, H_3, \dots, H_3),$$

and

$$|\vec{s}_i|^2 = \sum_{\mu=1}^n (s_i^\mu)^2, \quad (2.2)$$

while the pair interactions are given by

$$\mathcal{H}^1(\{\vec{s}_j\}) = \frac{1}{2} \sum_{(ij)} J_{ij} |\vec{s}_i - \vec{s}_j|^2. \quad (2.3)$$

The exchange parameters,  $J_{ij}$ , are positive and translation invariant and may conveniently be written<sup>8</sup>

$$J_{ij} = J_0 (a/R_0)^d \varphi(|R_{ij}|/R_0), \quad (2.4)$$

in which  $a$  is the lattice spacing and  $R_0$  represents the range of the interactions, while the shape function,  $\varphi(r)$ , is bounded for all  $r \geq 0$  and integrable on

$(0, \infty)$ . This form for  $J_{ij}$  includes the nearest-neighbor interactions when  $R_0$  is finite, and the long-range, infinitely weak, or van der Waals limit when  $R_0 \rightarrow \infty$ .

To obtain tricritical behavior, we take  $U < 0$  and  $V > 0$ , fixed in Eq. (2.1) and regard  $H$ ,  $H_3$ , and  $D$  as variable fields.<sup>8</sup>

In I we have shown that the model defined by Eqs. (2.1), (2.2), and (2.3) is exactly soluble in the limit  $n \rightarrow \infty$  and that it exhibits a tricritical point for  $d \geq 3$  (although not for  $d < 3$ ).<sup>8,9</sup> We may rescale the variables [see I Eq. (4.17)], to achieve the normalization

$$-U = V = 1. \quad (2.5)$$

If  $T_t$  is the tricritical temperature and one introduces the scaling fields [see I Eqs. (3.22), (4.6), (4.12), etc.]

$$t = (T - T_t)/T_t, \quad g = D - \frac{1}{4}(1 - t^2), \quad (2.6)$$

$$h = H + \frac{1}{2}(1 + t)H_3, \quad h_3 = H_3,$$

the tricritical point corresponds to  $t = g = h = h_3 = 0$ . One then finds [from I Eqs. (2.6), (3.8), (4.3), etc.] that the free energy in the tricritical region is given by

$$F(t, g, h, h_3) \approx F_0(t, g) + \min_{\tilde{m}} \left[ -\dot{p} \frac{\dot{\gamma}}{1 + \dot{\gamma}} \zeta^{1 + (1/\dot{\gamma})} - \frac{(h + h_3 \tilde{m})^2}{2\zeta} - \frac{1}{2} \zeta \tilde{m} + \frac{1}{2} g \tilde{m} + \frac{1}{4} t \tilde{m}^2 + \frac{1}{6} \tilde{m}^3 \right], \quad (2.7)$$

where  $\zeta = \zeta(\tilde{m}; \dot{p}; h, h_3)$  is the unique, nonnegative solution of the "constraint equation"

$$\tilde{m} = \left[ \frac{h + h_3 \tilde{m}}{\zeta} \right]^2 - \dot{p} \zeta^{1/\dot{\gamma}}, \quad (2.8)$$

while  $F_0$  represents an analytic background term [linear in  $g$  and cubic in  $t$ ; see I Eq. (4.16)]. In these equations the exponent  $\dot{\gamma}$  is the ordinary critical exponent of the susceptibility in the spherical model ( $n \rightarrow \infty$ ), namely,

$$\dot{\gamma} = 2/(d - 2), \quad (2.9)$$

for short-range interactions and  $d < 4$ , while  $\dot{p}$  is defined via the Fourier transform of the pair interactions (2.4) by

$$\dot{p} \equiv z = \frac{1}{2} J_0^{-1/\dot{\gamma}} b_{d,\varphi} (a/R_0)^d |U| V^{(d/6)-1}. \quad (2.10)$$

Here  $b_{d,\varphi}$  is a number which depends only on the shape function  $\varphi(r)$  and the dimensionality  $d$ . When

the range,  $R_0$ , of the interactions becomes infinite (the van der Waals limit),  $\dot{p}$  vanishes as  $R_0^{-d}$  and one sees immediately from Eqs. (2.7) and (2.8) that the free energy takes the form of a classical phenomenological free energy [see Appendix].

Of course, the minimization in Eq. (2.7) can be performed by differentiation. This leads to

$$\zeta + 2h_3(h + h_3\tilde{m})/\zeta = g + t\tilde{m} + \tilde{m}^2. \quad (2.11)$$

If one sets  $H = H_1$ ,  $D_2 = -2H_2$  and defines the three densities

$$m_l = \langle s^l \rangle = -(\partial F / \partial H_l) \quad (l = 1, 2, 3), \quad (2.12)$$

one finds [I Eqs. (3.17), (4.7), and (4.21)] the relations

$$m_1 \equiv m = \langle s \rangle = (h + h_3\tilde{m})/\zeta, \quad (2.13)$$

and

$$m_3 = m[\tilde{m} + \frac{1}{2}(1+t)] = mm_2. \quad (2.14)$$

The scaling properties of the free energy, Eq. (2.7), and the equations of state, (2.8) and (2.11), have been studied in some detail in Ref. 8. The main results are: (i) For  $3 < d < 4$ , tricritical scaling in its most direct form is impossible. To describe the complete tricritical region it is essential to recognize  $\dot{p} \propto (a/R_0)^d$  as a scaling variable. (ii) When  $\dot{p}$  is considered as a scaling variable, it scales with its own critical exponent,  $\phi_p = 3 - d$ . Evidently,  $\phi_p$  is negative for dimensionality  $d > 3$  and so  $\dot{p}$  is a "dangerous irrelevant variable". As expected,<sup>1</sup> the tricritical region is then characterized by *classical* tricritical exponents. (iii) In three dimensions ( $d = 3$ ) the exponent  $\phi_p$  vanishes identically, and it becomes possible to obtain a full scaling description using only the standard variables and the classical tricritical exponents. However, the variable  $\dot{p}$ , which is then marginal, enters the equation of state in a *nonuniversal* way.

In the following we restrict ourselves to the case  $d = 3$  (for which  $\dot{\gamma} = 2$ ) and study in detail the nonuniversal effects induced by  $\dot{p} \equiv z$  in the phase diagram. From Eqs. (2.7) to (2.12) we can then rewrite the free energy and equations of state near tricriticality as

$$F(t, g, h, h_3) \approx F_0(t, g) - \frac{2}{3}z\zeta^{3/2} - \frac{1}{2}(h + h_3\tilde{m})^2/\zeta - \frac{1}{2}\zeta\tilde{m} + \frac{1}{2}g\tilde{m} + \frac{1}{4}t\tilde{m}^2 + \frac{1}{6}\tilde{m}^3, \quad (2.15)$$

and

$$\tilde{m} = m^2 - z\zeta^{1/2}, \quad (2.16)$$

$$\zeta = g - 2h_3m + t\tilde{m} + \tilde{m}^2, \quad (2.17)$$

while the three densities,  $m_l$  ( $l = 1, 2, 3$ ), are still

given by Eqs. (2.13) and (2.14). Finally, note that when  $d = 3$  we have

$$z = c_0(a/R_0)^3, \quad (2.18)$$

where  $c_0$  and, hence,  $z$  is a pure number.

### III. PLANE OF SYMMETRY

Although a cubic or third-order (staggered) field,  $H_3$ , directly related to  $h$  in Eq. (2.6) may be induced experimentally in certain antiferromagnets like dysprosium aluminum garnet,<sup>5(b),(c)</sup>  $H_3$  is probably never independently accessible in magnetic systems. Furthermore, the best data currently available near tricritical points are taken in the symmetry plane where  $h = h_3 = 0$ . Indeed, for real systems like  $^3\text{He}$ - $^4\text{He}$  mixtures,<sup>4</sup> where neither  $h$  nor  $h_3$  can be generated, the symmetry plane fully represents the physically accessible space. It is thus such symmetric systems that we will have mainly in mind in this section, where we discuss the nonuniversal corrections induced by  $z$  for  $H \equiv H_3 = 0$ .

#### A. Triple line

The phase diagram for  $h = h_3 = 0$  is plotted on Fig. 1 of I. The lambda line above  $T_t$ , on which spherical model critical exponents occur, is given exactly by

$$g = D - D_t + \frac{1}{4}t^2 = 0 \quad (t \geq 0). \quad (3.1)$$

The lambda line continues smoothly into the triple line for  $T < T_t$ . Along the triple line disordered and ordered phases coexist: (i) the ordered phase is characterized by  $m \neq 0$  and  $\zeta = \partial h / \partial m = \chi^{-1} = 0$ , where  $\chi$  is the basic ordering susceptibility; (ii) the disordered phase has  $m = 0$  but  $\zeta > 0$ . In the *ordered* phase, therefore, Eqs. (2.16) and (2.17) reduce to

$$\tilde{m} = m^2, \quad \tilde{m}^2 + t\tilde{m} + g = 0. \quad (3.2)$$

The second equation has a unique, thermodynamically stable solution

$$\tilde{m}_{<}(t, g) = m_{<}^2(t, g) = -\frac{1}{2}[t - (t^2 - 4g)^{1/2}], \quad (3.3)$$

where, here and below, the subscript  $<$  denotes the *ordered phase*. Introducing Eq. (3.3) in Eq. (2.15) with  $\zeta = 0$ , one finds the free energy of the ordered phase in the symmetry plane. For  $t \leq 0$  one obtains

$$F_{<}(t, g) = F_0(t, g) - \frac{1}{24}|t|^3[1 - 6x + (1 - 4x)^{3/2}], \quad (3.4)$$

where we have introduced the tricritical scaling variable

$$x = g/|t|^2. \quad (3.5)$$

Note that  $F_{<}$  is independent of the nonuniversality

parameter  $z$ .

In the *disordered phase*, however, Eqs. (2.16) and (2.17) reduce to

$$\tilde{m} = -z\zeta^{1/2}, \quad \zeta = g + t\tilde{m} + \tilde{m}^2, \quad (3.6)$$

from which follows a quadratic equation for  $\zeta^{1/2}$ , namely,

$$(1-z^2)\zeta + zt\zeta^{1/2} - g = 0. \quad (3.7)$$

This has the thermodynamically stable solution

$$\zeta_{>}^{1/2} = -\frac{1}{2}(1-z^2)^{-1}[zt - [z^2t^2 + 4g(1-z^2)]^{1/2}]. \quad (3.8)$$

Note, however, that this is valid only for  $0 \leq z < 1$ ; for  $z \geq 1$  the model (for  $d=3$ ) no longer exhibits a tricritical point.<sup>8,10</sup> On introducing Eq. (3.8) into Eq. (2.15) with  $m=0$ , one obtains the free energy of the disordered phase for  $T \leq T_t$  ( $t < 0$ ) as

$$F_{>}(t, g; z) = F_0(t, g) - \frac{1}{24}|t|^3 c_z^{-2} \times [(1+6c_z x) + (1+4c_z x)^{3/2}], \quad (3.9)$$

where

$$c_z = (1-z^2)/z^2 \quad (3.10)$$

while  $>$  denotes the *disordered phase* (for which  $g > 0$  when  $t \geq 0$ ). Now, the triple line is the locus in the  $(t, g)$  plane where  $F_{<}(t, g) = F_{>}(t, g; z)$ , which yields

$$1 - 6x + (1 - 4x)^{3/2} = c_z^{-2}[(1 + 6c_z x) + (1 + 4c_z x)^{3/2}]. \quad (3.11)$$

The desired solution,  $x = x_r = g_r(t, z)/t^2$ , is one of the solutions of

$$x^3[x^3 - \frac{3}{8}(1 - c_z^{-1})x^2 + \frac{9}{256}(1 - \frac{1}{3}c_z^{-1})(1 - 3c_z^{-1})x + \frac{1}{128}c_z^{-1}(1 - c_z^{-1})] = 0, \quad (3.12)$$

obtained by squaring twice and rearranging. As  $c_z \neq \pm 1$  for  $0 \leq z \leq 1$ , one can exclude the solutions  $x=0$ . Of the remaining three solutions only

$$x_r(z) = \frac{1}{4}(1-z^2)^{-1}[\cos^2\phi(z) - z^2], \quad (3.13)$$

where

$$\phi(z) = \frac{1}{6}[\pi + \cos^{-1}(1 - 2z^2)], \quad (3.14)$$

is also a solution of Eq. (3.11). Hence, the triple line is given by

$$g_r(t; z) = \frac{1}{4}t^2(1-z^2)^{-1}[\cos^2\phi(z) - z^2]. \quad (3.15)$$

This expression is valid for small  $t \leq 0$  but for *all*  $z$  in the range  $0 \leq z < 1$ . When  $z=0$  one has  $\phi = \frac{1}{6}\pi$ , so that

$$g_r(t; z=0) = \frac{3}{16}t^2, \quad (3.16)$$

which is the result obtained in the classical theory [see Appendix, Eq. (A33)]. Note also that  $x_r(z)$ ,

and hence  $g_r(t; z)$ , decreases monotonically as  $z$  increases, vanishes for  $z=1/\sqrt{2}$ , and diverges as

$$x_r(z) \approx -3/32(1-z) \text{ as } z \rightarrow 1-. \quad (3.17)$$

Although  $g_r$  changes sign, the original quadratic field,  $(D - D_t)$ , is always negative on the triple line [see Eqs. (2.6) and (3.1)].

## B. Nonuniversal scaling functions

It is easy to derive explicit expressions for the scaling functions in the symmetry plane. Indeed, Eqs. (3.4) and (3.9) give the free energy scaling functions for  $t \leq 0$  in terms of the scaling variable  $x = g/t^2$ . In general one finds

$$F(t, g; z) = F_0(t, g) + |t|^{2-\alpha} \mathfrak{F}_{\pm}^{\pm}(g/t^2; z), \quad (3.18)$$

where  $\alpha = -1$  is the expected classical tricritical specific-heat exponent, while in the ordered region ( $<$ ) one has

$$\mathfrak{F}_{<}^{\pm}(x; z) = \pm \frac{1}{24}[1 - 6x \mp (1 - 4x)^{3/2}], \quad (3.19)$$

which is independent of  $z$ , and, in the disordered region ( $>$ )

$$\mathfrak{F}_{>}^{\pm}(x; z) = \pm \frac{z}{24(1-z^2)^2} \times \{z^3 + 6(1-z^2)zx \mp [z^2 + 4(1-z^2)x]^{3/2}\}, \quad (3.20)$$

The superscript, (+) or (−), in these expressions refers to  $t > 0$  or  $t < 0$ , respectively. Note that the free energy expressions are analytic in  $t$  through  $t=0$  for  $g > 0$  and  $g < 0$ , as they should be.

Of particular interest in the symmetry plane are the nonordering density  $m_2$  (or  $\tilde{m}$ ) and the corresponding nonordering susceptibility

$$\tilde{\chi} \equiv \chi_2 = \frac{1}{2}(\partial m_2 / \partial H_2)_T = -(\partial \tilde{m} / \partial g)_t. \quad (3.21)$$

These quantities have direct physical interpretations: for an antiferromagnet,  $-m_2$  is essentially the ordinary magnetization,  $M$ , while  $\tilde{\chi}$  is proportional to the ordinary magnetic susceptibility  $\chi_T = (\partial M / \partial H)_T$ ; in  $^3\text{He}$ - $^4\text{He}$  mixtures  $-m_2$  represents the molar concentration,  $x_3$ , of  $^3\text{He}$ , whereas  $\tilde{\chi}$  is the concentration susceptibility  $(\partial x_3 / \partial \Delta)_T$ , where  $\Delta = \mu_3 - \mu_4$  is the chemical potential difference.

The scaling function for  $m_2$  is obtained by introducing Eq. (3.3) or (3.8) in Eqs. (2.14) and (2.16). One finds

$$\tilde{m}(t, g; z) = m_2 - \frac{1}{2}(1+t) = |t|^{\tilde{\beta}} Q_{\pm}^{\pm}(g/t^2; z), \quad (3.22)$$

where  $\tilde{\beta} = \beta_2 = 1$ , and

$$Q_{<}^{\pm}(x; z) = \mp \frac{1}{2} + \frac{1}{2}(1 - 4x)^{1/2}, \quad (3.23)$$

while, in the disordered region,

$$Q_{>}^{\pm}(x; z) = \pm \frac{1}{2} \frac{z}{1 - z^2} [z + [z^2 \mp 4(1 - z^2)x]^{1/2}]. \quad (3.24)$$

Alternatively, one may rewrite Eq. (3.22) using  $g$  as a scaling variable, as

$$\begin{aligned} \tilde{m}(t, g; z) &\equiv m_2 - \frac{1}{2}(1 + t) \\ &= |g|^{\tilde{\beta}_t} \tilde{Q}_{\geq}(t/|g|^{1/2}; z), \end{aligned} \quad (3.25)$$

with  $\tilde{\beta}_t = \tilde{\beta}/\phi = \frac{1}{2}$  and

$$\tilde{Q}_{>}(w; z) = \frac{1}{2} \frac{z}{1 - z^2} [zw - [w^2 z^2 \pm 4(1 - z^2)]^{1/2}], \quad (3.26)$$

$$\tilde{Q}_{<}(w; z) = -\frac{1}{2} w + \frac{1}{2} (w^2 \mp 4)^{1/2}, \quad (3.27)$$

where the signs  $(-)$  and  $(+)$  apply for  $g \geq 0$ , respectively.

By differentiation the susceptibility is found to scale as

$$\tilde{\chi}(t, g; z) = |t|^{-\tilde{\gamma}} X_{\geq}(g/t^2; z), \quad (3.28)$$

where  $\tilde{\gamma} = 1$  and

$$X_{<}(x; z) = (1 - 4x)^{-1/2}, \quad (3.29)$$

$$X_{>}(x; z) = z [z^2 + 4(1 - z^2)x]^{-1/2}. \quad (3.30)$$

Again one can rewrite the scaling in terms of  $g$  with a prefactor  $|g|^{-\tilde{\gamma}_t}$  where  $\tilde{\gamma}_t = \tilde{\gamma}/\phi = \frac{1}{2}$ .

From the explicit expressions presented above, one sees that the scaling functions in the *ordered* phase on the symmetry plane are independent of  $z$  and, hence, universal. In the *disordered* phase, however, the scaling functions depend explicitly on  $z$  and so are nonuniversal. On the other hand, scaling is clearly verified for  $z > 0$ , and all the exponents take the expected classical values. This is not actually true in the  $(z = 0)$  classical theory. Indeed, the disordered phase scaling functions (3.20), (3.24), (3.26), and (3.30) vanish identically when  $z = 0$ . The leading asymptotic behavior is then given by correction-to-scaling terms and described by different exponents in the ordered and disordered phases. This peculiarity has, of course, been commented on before.<sup>11</sup>

### C. Physical fields

As one can see in Fig. 1 of I, or by inspecting Eqs. (3.1) and (3.15), the lambda line,  $g_{\lambda}(t)$ , and the triple line  $g_{\tau}(t; z)$  have zero slope at the tricritical point. This behavior merely reflects the fact that  $t$  and  $g$ , as

defined in Eq. (2.6), respect the appropriate scaling axes<sup>12-14</sup> near the tricritical point. In real systems,<sup>4-6</sup> however, the slope of the phase boundary is normally nonzero at tricriticality. Thus, in applications of the Hamiltonian (2.1) or the free energy (2.7), one should not expect the physical fields to be proportional to the scaling variables, but rather to be linear combinations (at least asymptotically) of the scaling variables. To explore the consequences of this, we will regard  $H_2$  or  $h_2$ , with

$$h_2 - h_{2,t} \equiv g - qt = g_0 - qt + \frac{1}{4}t^2, \quad (3.31)$$

as the physical field rather than  $g$ . One easily sees that the slope of the lambda line  $T_{\lambda}(h_2)$  at tricriticality is then given by

$$\left. \frac{dT_{\lambda}}{dh_2} \right|_{T=T_t} = -\frac{1}{q}. \quad (3.32)$$

We can now use Eqs. (3.22) to Eq. (3.30) to examine the asymptotic behavior of  $m_2$  and  $X_2 = \tilde{\chi}$  along different loci in the plane of the physical fields  $(T, H_2)$ . We will define various dimensionless amplitude ratios which are accessible to experiment but which depend on  $z$  and are hence nonuniversal.

### D. Nonuniversal amplitude ratio for the phase boundary

Consider first the behavior of  $m_2$  when the tricritical point is approached along the phase boundaries as illustrated in Fig. 1. On the lambda line one has, by

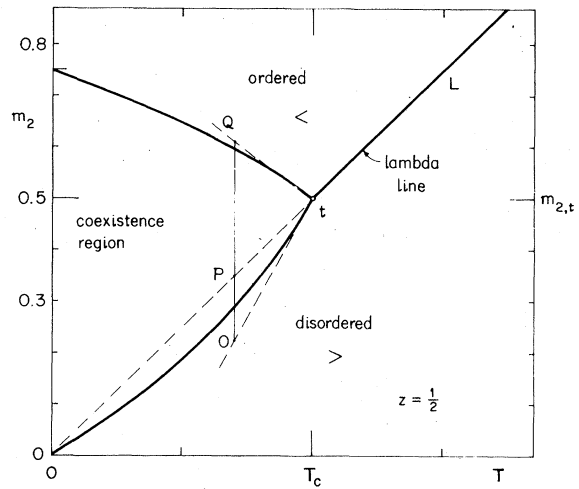


FIG. 1. Tricritical phase diagram in the  $(m_2, T)$  plane in the limit  $n \rightarrow \infty$  with nonuniversality parameter  $z = \frac{1}{2}$  (obtained by solving the exact equations of state). The dashed lines  $Ot$ ,  $Pt$ , and  $Qt$  indicate the asymptotic slopes of the phase boundaries above and below the tricritical point. Note that the disordered phase boundary exhibits a discontinuity in slope at the tricritical point (except in the van der Waals or classical limit  $z = 0$ ).

Eq. (3.1),  $t > 0$  and  $g = 0$  so that Eq. (3.22) yields

$$m_{2,\lambda}(T) - m_{2,t} \approx A_\lambda t, \quad \text{with } A_\lambda = \frac{1}{2}, \quad (3.33)$$

where  $m_{2,t} = \frac{1}{2}$ . Note that, since the phase transition is continuous on the lambda line, there is no need to distinguish between  $m_2^>$  and  $m_2^<$ . On the triple line, however, two phases with different values of  $m_2$  coexist. Inserting Eq. (3.15) with  $t < 0$  into Eq. (3.22) yields

$$m_{2,\tau}^>(T; z) - m_{2,t} \approx A_{\tau>} t, \quad (3.34)$$

with

$$A_{\tau>} = \frac{1}{2} \left( 1 + \frac{z}{1-z^2} [z + [z^2 + 4(1-z^2)x_\tau]^{1/2}] \right), \quad (3.35)$$

$$A_{\tau<} = -\frac{1}{2} (1 - 4x_\tau)^{1/2},$$

where  $x_\tau(z)$  is given explicitly by Eq. (3.13).

Evidently the slopes for  $m_{2,\lambda}$  and  $m_{2,\tau}^>$ , following from Eqs. (3.33) and (3.34), are unequal unless  $z = 0$ . Hence, as illustrated in Fig. 1, the slope of the disordered side of the phase boundary in the  $(m_2, T)$  plane, i.e., the locus  $OL$ , is *discontinuous* at the tricritical point; this is in marked contrast to the classical or mean-field prediction of continuity. As emphasized in Ref. 7, a discontinuity in slope is observed in real systems.<sup>4,5</sup> It has also been seen in series extrapolations<sup>15</sup> and Monte Carlo calculations<sup>16</sup> for the Blume-Capel model.<sup>17</sup>

The discontinuity in slope can be characterized in dimensionless form<sup>7</sup> by the ratio

$$\mathfrak{Q}_1(z) = \frac{[OP]}{[PQ]} = \frac{A_{\tau>} - A_\lambda}{A_\lambda - A_{\tau<}}, \quad (3.36)$$

where the lengths  $[OP]$  and  $[PQ]$  measure the difference in asymptotic slopes at the tricritical point as indicated in Fig. 1. From Eqs. (3.33) – (3.35) and (3.13) one finds,<sup>7</sup> after some trigonometric manipulations,

$$\begin{aligned} \mathfrak{Q}_1(z) &= \frac{z}{(1-z^2)^{1/2}} \tan \phi(z) \\ &= \tan \theta(z) \tan \left[ \frac{1}{3} \left( \theta + \frac{1}{2} \pi \right) \right], \end{aligned} \quad (3.37)$$

where we have introduced the more simply defined angle

$$\theta(z) = 3\phi(z) - \frac{1}{2}\pi = \sin^{-1} z. \quad (3.38)$$

For small  $z$  one has

$$\mathfrak{Q}_1(z) = \frac{1}{\sqrt{3}} z + \frac{4}{9} z^2 + \frac{35}{54\sqrt{3}} z^3 + O(z^4). \quad (3.39)$$

Evidently the discontinuity in slope is nonuniversal

but is governed by the single range parameter  $z$ . The ratio  $\mathfrak{Q}_1$  is monotonic increasing in  $z$  and, as expected, vanishes in the van der Waals limit,  $z \rightarrow 0$ . Conversely,  $\mathfrak{Q}_1$  diverges as  $\sqrt{3}/2(1-z)^{1/2}$  when  $z \rightarrow 1$ ; this is symptomatic of the fact that the model displays no tricritical point for  $z > 1$ .

#### E. Nonordering susceptibility: nonuniversal amplitude ratios

Other clear tests of nonuniversality are provided by examining the nonordering susceptibility  $\chi_2 \equiv \tilde{\chi}$  on various loci. On the tricritical isotherm,  $T = T_t$ , the scaling field  $g$  is identical to  $h_2 - h_{2,t}$ , and one may write

$$\chi_2(T_t, h_2; z) \approx B_{\geq}(z) / |h_2 - h_{2,t}|^{1/2}, \quad \text{for } g \gtrless 0, \quad (3.40)$$

as follows from Eq. (3.28). Then, from Eqs. (3.29) and (3.30), one finds that the corresponding dimensionless amplitude ratio is

$$\mathfrak{Q}_2(z) = \frac{B_{>}}{B_{<}} = \frac{z}{(1-z^2)^{1/2}} \equiv \tan \theta(z). \quad (3.41)$$

Evidently this ratio also vanishes only in the van der Waals limit  $z \rightarrow 0$ .

On the critical "isochamp",  $h_2 = h_{2,t}$ , one has  $g = -qt$  so that from Eq. (3.28) one can write

$$\chi_2(T, h_{2,t}; z) \approx C_{\geq}(z) / |t|^{1/2}, \quad (3.42)$$

where, as before  $>$  and  $<$  refer to the disordered and ordered phases, respectively. The corresponding amplitude ratio is

$$\mathfrak{Q}_3(z) = \frac{C_{>}}{C_{<}} = \frac{z}{(1-z^2)^{1/2}} \equiv \tan \theta(z), \quad (3.43)$$

and is independent of  $q$  although  $C_{>}$  and  $C_{<}$

separately vary as  $|q|^{-1/2}$ . Note that  $\mathfrak{Q}_3$  is identically equal to  $\mathfrak{Q}_2(z)$ ; however, this equality is purely a consequence of the fact that scaling holds with a crossover exponent  $\phi (=2) > 1$ .

Finally, if the tricritical point is approached along the two sides of the triple line, one finds from Eq. (3.28) that

$$\chi_2(T, h_{2,\tau} z) \approx G_{\geq}(z) / |t|, \quad (3.44)$$

where the amplitudes follow from the scaling functions (3.29) and (3.30) by inserting the triple line value  $x_\tau(z)$ . For the appropriate dimensionless ratio

one thus discovers

$$\mathfrak{Q}_4(z) = \frac{G_>}{G_<} = \frac{z}{(1-z^2)^{1/2}} \tan \phi(z) \quad (3.45)$$

This happens to be identical to  $\mathfrak{Q}_1(z)$  [see Eq. (3.37) above]; however, the result is nontrivial and *not* merely a consequence of scaling.

In summary, we have defined and computed in the symmetry plane (for the  $n \rightarrow \infty$  limit) four nonuniversal dimensionless amplitude ratios,  $\mathfrak{Q}_j$ . Within classical theory, which is realized in the van der Waals limit  $z \rightarrow 0$ , all these ratios vanish (and are thus trivially universal). Since there is only a single nonuniversality parameter, namely  $z \propto (a/R_0)^d$ , a measurement of one of the ratios  $\mathfrak{Q}_j(z)$  for a given system serves to determine  $z$ . The remaining ratios may then be predicted. In other words, even though the various ratios are nonuniversal, a definite relation holds between any pair of them. The ratios  $\mathfrak{Q}_j$  are accessible to experiments on antiferromagnets and  $^3\text{He}$ - $^4\text{He}$  mixtures and are observed to take nonclassical and nonuniversal values. As demonstrated in Ref. 7, the predicted ratio relations are also found to be obeyed surprisingly well: indeed, within the precision of current experimental data there are no discrepancies! However, it must be stressed that this agreement is theoretically puzzling since, in the first instance, real systems should be described by finite and small values of  $n$  and not by  $n \rightarrow \infty$ . In the second place, for  $n < \infty$  various logarithmic factors are expected in the asymptotic behavior on the different loci<sup>1,3</sup> but such factors have not been allowed for in our definitions of the amplitudes. Hence the meaning, and even the existence of the ratios  $\mathfrak{Q}_j$  for general  $n$  is not obvious: see further in Sec. V below.

#### F. Locus-dependent amplitudes

To conclude this section, we mention that Riedel *et al.*<sup>4(b)</sup> have exhibited certain nonuniversal ratios for tricritical behavior within a phenomenological scaling theory. However, their amplitude ratios are nonuniversal in the sense that they depend on the direction of approach to the tricritical point relative to the direction singled out by the lambda line. As the model (2.1) satisfies the assumptions of tricritical scaling formulated by Riedel *et al.*,<sup>4(b)</sup> we should be able to calculate the same amplitude ratios.

To check the point, we examine the amplitudes of  $\tilde{m}$  [which corresponds to  $X^{\text{sing}}$  in Ref. 4(b)] and of  $\chi_2$  [which corresponds to  $(\partial X^{\text{sing}}/\partial \beta_T \Delta)_T$  in Ref. 4(b)] when the tricritical point is approached along the path

$$h_2 - h_{2,t} = q't, \quad (3.46)$$

in the symmetry plane. On such a locus one has  $g = (q + q')t$ , and from Eqs. (3.25) and (3.28) one

finds

$$\begin{aligned} \tilde{m}_{\geq}(t, g; z) &\approx |q + q'|^{1/2} |t|^{1/2} \tilde{Q}_{\geq}^{\pm}(0) \\ &= \tilde{A}_{\geq}(q') |t|^{1/2}, \end{aligned} \quad (3.47)$$

$$\begin{aligned} \chi_{2\geq}(t, g; z) &\approx |q + q'|^{-1/2} |t|^{-1/2} \tilde{X}_{\geq}^{\pm}(0) \\ &= B_{\geq}(q') |t|^{-1/2}, \end{aligned} \quad (3.48)$$

where  $\tilde{X}_{\geq}^{\pm}(w)$  denotes the scaling functions in terms of  $w = t/|g|^{1/2}$ . Note that along a path such as (3.46) one has  $g < 0$  in the ordered phase close enough to the tricritical point, and  $g > 0$  in the disordered phase. The amplitudes  $\tilde{A}_{\geq}$  and  $B_{\geq}$  correspond

to  $A_X$  and  $A_Y$  of Riedel *et al.*, respectively. Using Eqs. (3.26), (3.27), (3.29), and (3.30), one can compute the ratios  $B_{\geq}/\tilde{A}_{\geq}$  and  $B_{\leq}/\tilde{A}_{\leq}$  with the result

$$\begin{aligned} \frac{|B_{\geq}(q')|}{|\tilde{A}_{\geq}(q')|} &= \frac{1}{2} |q + q'|^{-1} \\ &= \frac{1}{2} \frac{1}{|q|} \left| 1 + \frac{q'}{q} \right|^{-1}. \end{aligned} \quad (3.49)$$

In particular, if  $q' = 0$  and  $q' = 1$ , one obtains, using Eq. (3.32),

$$\frac{|B(0)|}{|\tilde{A}(0)|} = \frac{1}{2} \left| \left( \frac{dT_{\lambda}}{dh_2} \right)_t \right|, \quad (3.50)$$

$$\frac{|B(1)|}{|\tilde{A}(1)|} = \frac{1}{2} \left| \left( \frac{dT_{\lambda}}{dh_2} \right)_t \right| \left| 1 - \left( \frac{dT_{\lambda}}{dh_2} \right)_t \right|^{-1}, \quad (3.51)$$

which are the analogs of the relations (25) and (29) of Ref. 4(b). Note that these amplitude ratios are not "naturally" dimensionless in the sense that they involve amplitudes for distinct physical quantities. Furthermore, these ratios, although path dependent, do *not* depend on the nonuniversality parameter,  $z$ .

#### IV. FULL THREE-PHASE REGION

We consider now the tricritical region in the full space of four fields  $(t, g, h, h_3)$ . In particular, we focus on the three-phase region in density space for fixed  $T < T_t$  ( $t < 0$ ). In the field space,  $(t, g, h, h_3)$ , this is represented by the triple surface. [See Fig. 2 which exhibits  $(g, h)$  sections of the classical phase diagram ( $z = 0$ ).] In classical theory,<sup>2,18</sup> the three-phase region in the density space,  $(m_1, m_2, m_3)$ , fills a volume bounded by a single ruled surface of interesting shape, namely, the three-phase monohedron (see, e.g., Fig. 2 of Ref. 7 and the Appendix). The three-phase

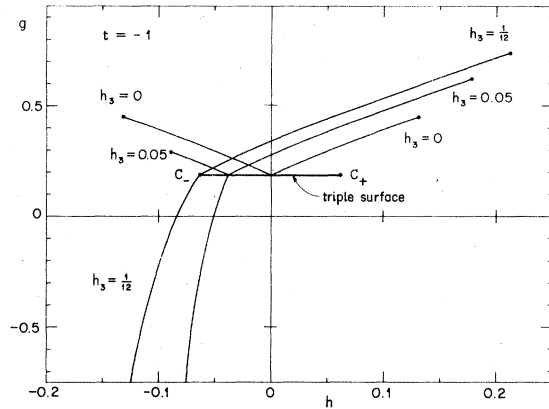


FIG. 2. A  $(g, h)$  section of the classical tricritical phase diagram in  $(t, g, h)$  space for fixed  $t = -1$  and for  $h_3 = 0, 0.05$ , and  $\frac{1}{12}$  showing the first-order wing surfaces;  $C_+$  and  $C_-$  denote the critical end-points, while the line  $C_+C_-$  represents the triple surface.

monohedron has also been studied in real fluid systems.<sup>6</sup> When  $H_3$  is allowed to be nonzero, the model defined by Eq. (2.1) is appropriate for describing ternary and quaternary liquid mixtures: then  $m_1$ ,  $m_2$ , and  $m_3$  represent suitable linear (but temperature varying) combinations of the various compositions, while  $H_1 = H$ ,  $H_2 = -\frac{1}{2}D$ , and  $H_3$  denote corresponding linear combinations of the chemical potentials  $\mu_1$ ,  $\mu_2$ ,  $\mu_3$  (and  $\mu_4$  in the case of quaternary mixtures). The classical theory provides a reasonably good description of current experimental observations,<sup>6</sup> although some discrepancies are indicated. However, it is, in any case, instructive to examine the three-phase region in the infinite-component limit with  $z \equiv \bar{p}$  different from zero, in order to discover the nonuniversal nonclassical modifications of the monohedron.

When  $H$  and  $H_3$  are both nonzero, we have, unfortunately, been unable to obtain an exact, explicit representation of the three-phase region for all values of  $z$  in the range  $0 \leq z < 1$  (as was achieved in Sec. III). Accordingly, we present here an analysis valid for general  $h$  and  $h_3$  but limited to first order in small  $z$ . The basis of the calculations will be the classical or  $z = 0$  theory, expounded in the Appendix.

#### A. First-order expansion in $z$

To start, we rewrite Eqs. (2.15)–(2.17) in a form which is more convenient for expansion around  $z = 0$ . Using Eq. (2.16) to substitute for  $\bar{m}$  in Eqs. (2.15) and (2.17) and neglecting terms of order  $z^2$

and higher yields, for  $t < 0$ ,

$$F(t, g, h, h_3) \approx F_0(t, g) - hm + \frac{1}{2}gm^2 - h_3m^3 - \frac{1}{4}|t|m^4 + \frac{1}{6}m^6 - \frac{1}{2}z\zeta^{1/2}(m^4 - |t|m^2 - 2h_3m + g) + \frac{1}{6}z\zeta^{3/2}, \quad (4.1)$$

where  $m$  satisfies

$$m^5 - |t|m^3 - 3h_3m^2 + gm - h \approx \frac{1}{2}z\zeta^{1/2}(4m^3 - 2|t|m - 2h_3). \quad (4.2)$$

Moreover, Eq. (2.13) reduces to a quadratic equation for  $\zeta^{1/2}$ , namely,

$$m\zeta + h_3z\zeta^{1/2} - (h + h_3m^2) = 0, \quad (4.3)$$

which has the unique, physically stable solution

$$\zeta(m) = (h + h_3m)/m + O(z). \quad (4.4)$$

On dividing both sides of Eq. (4.2) by  $m$  and rearranging, one obtains

$$m^4 - |t|m^2 - 2h_3m + g = \zeta(m) + O(z). \quad (4.5)$$

Introducing Eq. (4.5) in Eq. (4.1) yields, correct to  $O(z)$ ,

$$F(t, g, h, h_3; z) = F_0(t, g) - hm + \frac{1}{2}gm^2 - h_3m^3 - \frac{1}{4}|t|m^4 + \frac{1}{6}m^6 - \frac{1}{3}z\zeta^{3/2}(m). \quad (4.6)$$

This equation with Eq. (4.2) will serve as a basis for an expansion around  $z = 0$ ; it should be compared with Eqs. (A1) and (A2) of the Appendix.

In the following, to analyze the triple surface (for  $t < 0$ ), we choose  $t$  and  $m \equiv a \equiv m_0$  as independent variables: see Eqs. (A28) to (A34). To find the leading corrections to classical theory we then postulate the expansions

$$m_{\tau \pm}(t, m_0; z) = M_{\pm}(t, m_0) + zm'_{\pm}(t, m_0) + O(z^2), \quad (4.7)$$

and

$$g_{\tau}(t, m_0; z) = \frac{3}{16}t^2 + zg'(t, m_0) + O(z^2), \quad (4.8)$$

$$h_{\tau}(t, m_0; z) = -\frac{1}{4}|t|m_0(m_0^2 - \frac{3}{4}|t|) + zh'(t, m_0) + O(z^2), \quad (4.9)$$

$$h_{3, \tau}(t, m_0; z) = \frac{1}{3}m_0(m_0^2 - \frac{3}{4}|t|) + zh'_3(t, m_0) + O(z^2), \quad (4.10)$$

where the zero-order term,  $M_{\pm}(t, m_0)$ , is given explicitly by Eq. (A30), while Eqs. (A32) to (A34) have been quoted for the zero-order values of  $g$ ,  $h$ , and  $h_3$  on the triple surface (denoted by the subscript  $\tau$ ).

Now on the triple surface the magnetizations



$m = m_0$ ,  $m_+$ , and  $m_-$  must yield equal minima of the free energy so that we have the equations

$$\mathcal{F}(m_0; t, g_\tau, h_\tau, h_3, \tau; z) = \mathcal{F}(m_\pm; t, g_\tau, h_\tau, h_3, \tau; z) , \quad (4.11)$$

where  $\mathcal{F}(m; t, h, h_3; z)$  denotes the expression on the right-hand side of Eq. (4.6). On introducing Eqs. (4.7) to (4.10) into this relation and Eq. (4.2), and recalling that  $m_\pm = M_\pm$  solves the equations to zero order in  $z$ , we obtain a system of five linear equations for the five unknowns,  $m'_+$ ,  $m'_-$ ,  $g'$ ,  $h'$ , and  $h'_3$ , namely:

$$\frac{1}{2} M_\pm g' + h' + \frac{3}{4} |t| h'_3 = \mathcal{L}(M_\pm) , \quad (4.12)$$

$$m_0 g' - h' - 3 m_0^2 h'_3 = \mathcal{K}(m_0) , \quad (4.13)$$

$$M_\pm g' - h' - 3 M_\pm^2 h'_3 + 3 (M_\pm^2 - \frac{1}{4} |t|) m'_\pm = \mathcal{K}(M_\pm) , \quad (4.14)$$

where the auxiliary functions are

$$\mathcal{L}(M) = \frac{|M^2 - \frac{3}{4} |t||^3 - |m_0^2 - \frac{3}{4} |t||^3}{9\sqrt{3}(m_0 - M)} , \quad (4.15)$$

$$\mathcal{K}(M) = \frac{5}{3\sqrt{3}} M (M^2 - \frac{9}{20} |t|) |M^2 - \frac{3}{4} |t|| . \quad (4.16)$$

In deriving the expressions for  $\mathcal{L}(M)$  and  $\mathcal{K}(M)$ , we have used the expression (4.4) for  $\zeta(m)$  and noted that, on the triple surface,

$$\begin{aligned} \xi^{1/2}(M) &= (h + h_3 M^2)^{1/2} / M^{1/2} + O(z) , \\ &= |M^2 - \frac{3}{4} |t|| / \sqrt{3} + O(z) , \end{aligned} \quad (4.17)$$

where the zero-order values of  $h$  and  $h_3$  on the triple surface as given by Eqs. (4.9) and (4.10) have been employed.

This system of equations is easily reduced to the triangular form

$$g' = -2[\mathcal{L}(M_+) - \mathcal{L}(M_-)] / (M_+ - M_-) , \quad (4.18)$$

$$h'_3 = \frac{1}{3} (m_0^2 - \frac{1}{4} |t|)^{-1} [(m_0 + \frac{1}{2} M_-) g' - \mathcal{L}(M_+) - \mathcal{K}(m_0)] , \quad (4.19)$$

$$h' = m_0 g' - 3 m_0^2 h'_3 - \mathcal{K}(m_0) , \quad (4.20)$$

and

$$m'_\pm = \frac{1}{3} (M_\pm^2 - \frac{1}{4} |t|)^{-2} [\mathcal{K}(M_\pm) - M_\pm g' + h' + 3 M_\pm^2 h'_3] . \quad (4.21)$$

For most of the subsequent computations these equations are fairly convenient as they stand. However, an explicit solution is straightforward, although rather tedious. The final results are most compactly expressed in terms of the scaled variable

$$w = m_0 / |t|^{1/2} , \quad (4.22)$$

where the range  $0 \leq w^2 \leq \frac{3}{4}$  (or  $m_0^2 \leq \frac{3}{4} |t|$ ) covers the whole three-phase region for  $t < 0$ . For brevity we also write

$$\begin{aligned} \Delta(w) &= (1 - w^2)^{1/2} \\ &= (|t| - m_0^2)^{1/2} / |t|^{1/2} . \end{aligned} \quad (4.23)$$

Then we obtain

$$g'(t, m_0) = -\frac{t^2}{8\sqrt{3}} (1 - 4w^2)^{-1} \left[ (1 - \frac{4}{3} w^2)^3 - \frac{8|w|^3}{3\sqrt{3}\Delta} (1 + 2w^2 - \frac{8}{3} w^4) \right] , \quad (4.24)$$

$$h'(t, m_0) = \frac{7|t|^{5/2}}{16\sqrt{3}} \frac{w}{(1 - 4w^2)^2} \left[ P_1(w) + \frac{16|w|^3}{21\sqrt{3}\Delta} P_2(w) \right] , \quad (4.25)$$

$$h'_3(t, m_0) = -\frac{|t|^{3/2}}{2\sqrt{3}} \frac{w}{(1 - 4w^2)^2} \left[ P_3(w) + \frac{2|w|^3}{\sqrt{3}\Delta} P_4(w) \right] , \quad (4.26)$$

and, finally,

$$m'_\pm(t, m_0) = \pm \frac{|t|^{1/2}}{12} \frac{[P_5(w)\Delta \mp 2\sqrt{3}wP_6(w) + 2\sqrt{3}|w|P_7(w) \pm 2w|w|P_8(w)/\Delta]}{\Delta^2(w)(1 - 4w^2)^3} , \quad (4.27)$$

where the  $P_j(w)$  are polynomials in  $w^2$  of the form

$$P_j(w) = 1 + \sum_{k=1}^4 p_{jk} w^{2k} , \quad (4.28)$$

whose coefficients are given explicitly in Table I. The reader may check explicitly that the square-bracketed terms in Eqs. (4.24)–(4.27) vanish as fast as the terms  $(1 - 4w^2)^l$  in the denominators, so that  $g'$ ,  $h'$ ,  $h'_3$ , and  $m'_\pm$  all

TABLE I. Coefficients  $p_{jk}$  for the polynomials  $P_j(w)$  defining the first-order nonclassical terms.

$j$	$k=1$	$k=2$	$k=3$	$k=4$
1	-64/7	160/7	-3328/189	256/189
2	7	-40/3	16/3	0
3	-28/3	208/9	-448/27	0
4	-8/27	-16/27	0	0
5	-14	328/3	-7264/27	5248/27
6	-47/3	500/9	-1936/27	832/27
7	-139/9	508/9	-80	320/9
8	-101/3	1276/9	-1808/9	832/9

remain finite as  $w$  passes through the values  $\pm \frac{1}{2}$  (where  $m_0 = \pm \frac{1}{2}|t|^{1/2}$ ). However, it should be noted that the expressions are *nonanalytic* in  $w$  at  $w=0$ , i.e., at the plane of symmetry ( $m_0=0$ ). This nonanalyticity will be discussed in more detail below.

#### B. Canonical form for the monohedron

The knowledge of the coefficients (4.24) to (4.27) is sufficient to specify the whole three-phase monohedron to first order in  $z$ . In fact, on introducing Eq. (4.27) into Eq. (4.7) and using Eqs. (4.17), (2.13), (2.14), and (2.16) one can compute the values of  $m_2$  and  $m_3$  to first order in  $z$  for each value of  $m_0$  and  $t$ . However, a glance at Eqs. (2.12)–(2.14) shows that the simple relations (A42), namely,  $m_2 = m_1^2$ , and  $m_3 = m_1^3$ , are not obeyed as soon as  $z \neq 0$ . Indeed, in a space in which the  $m_j$  are chosen as orthonormal axes the edge of the monohedron will have a more complicated, "twisted" form. In order to compare most readily with classical theory, we thus introduce the new scaled combinations

$$w_1 = m/|t|^{1/2} \equiv w, \quad (4.29)$$

$$w_2 = \tilde{m}/|t| = [m_2 - \frac{1}{2}(1+t)]/|t|, \quad (4.29)$$

$$w_3 = m[(1-\psi)\tilde{m} + \psi]/|t|^{3/2}, \quad (4.30)$$

where the identity  $m \equiv m_0$  should be recalled. We choose  $\psi(z)$ , the mixing coefficient for  $w_3$ , so that the edge of the monohedron, projected onto the  $(w_1, w_3)$  plane, is tangent to the  $w_1$  axis at the origin. If one uses Eqs. (2.14) and (4.17), one finds this condition is satisfied when

$$\begin{aligned} \psi(z) &= z \zeta^{1/2}(m=0) + O(z^2) \\ &= \frac{1}{4}\sqrt{3}z + O(z^2). \end{aligned} \quad (4.31)$$

Finally, using Eqs. (2.16), (4.17), and (4.31), one

can express  $w_2$  and  $w_3$  explicitly in terms of  $w$  as

$$w_2 = w^2 - \frac{1}{3}\sqrt{3}z|w^2 - \frac{3}{4}|, \quad (4.32)$$

$$\begin{aligned} w_3 &= (1 - \frac{1}{4}\sqrt{3}z)w(w_2 + \frac{1}{4}\sqrt{3}z) + O(z^2) \\ &= (1 - \frac{1}{4}\sqrt{3}z)w^3 \\ &\quad - \frac{1}{3}\sqrt{3}zw(|w^2 - \frac{3}{4}| - \frac{3}{4}) + O(z^2). \end{aligned} \quad (4.33)$$

The definition (4.29) of  $w_1$ , the expression (4.27) for  $m_{\pm}$  together with Eq. (4.7), and these last relations determine the edge of the three-phase monohedron to first order in  $z$  as a function of  $m_0$  and  $t$  (in the range  $m_0^2 \leq \frac{3}{4}|t|$ ), or, equivalently, of the scaled variable  $w = m_0/|t|^{1/2}$  ( $w^2 \leq \frac{3}{4}$ ). The relations (4.32) and (4.33) may be compared with the classical relations (A50) which are reproduced when  $z \rightarrow 0$ .

In the following we will use the foregoing results to study the characteristics of the three-phase monohedron in more detail and will specifically examine the departures from classical theory near the symmetry plane and in the vicinity of the critical end-points.

#### C. Vicinity of the symmetry plane

In terms of the scaled variable  $w = m/|t|^{1/2}$  (with  $m \equiv m_0$ ) the symmetry plane ( $h = h_3 = 0$ ) is characterized by  $w = 0$ . From Eqs. (4.24)–(4.27), therefore, the nonordering field and the densities on the symmetry plane are

$$g_0(z) = \frac{3}{16}t^2 \left( 1 - \frac{2}{3\sqrt{3}}z + O(z^2) \right), \quad (4.34)$$

which agrees with Eq. (3.15), and

$$\begin{aligned} m_{\pm}(t; m_0=0) &\equiv m_{0\pm}(t) \\ &= \pm \frac{1}{2}\sqrt{3}|t|^{1/2} \left( 1 + \frac{z}{6\sqrt{3}} + O(z^2) \right). \end{aligned} \quad (4.35)$$

From this, with Eqs. (4.29) and (4.30), one finds the vertices in density space of the "central" coexistence triangle,  $O_+OO_-$ , associated with the symmetry plane to first order in  $z$ : see Figs. 4–6 in the Appendix and Figs. 2 and 3 of Ref. 7. To first order in  $z$  the coordinates are found to be

$$O: (w_1, w_2, w_3)_O = (0, -\frac{1}{4}\sqrt{3}z, 0), \quad (4.36)$$

$$\begin{aligned} O_{\pm}: (w_1, w_2, w_3)_{O\pm} &= (\pm \frac{1}{2}\sqrt{3}, \frac{3}{4}, \pm \frac{3}{8}\sqrt{3}) \\ &\quad + (\pm \frac{1}{12}, \pm \frac{1}{12}\sqrt{3}, \pm \frac{9}{32}z). \end{aligned} \quad (4.37)$$

Small values of  $w$  correspond to small departures from the symmetry plane. Accordingly, in order to study the neighborhood of the symmetry plane, we expand the general expressions in powers of  $w$ . From Eqs. (4.24)–(4.27) or, in stages, from Eqs. (4.18) to (4.21) we obtain the triple surface as

$$\frac{g_\tau(w; z) - g_0(z)}{t^2} = \frac{1}{9} z |w|^3 - \frac{2}{9} \sqrt{3} z w^4 + O(z w^5), \quad (4.38)$$

$$\begin{aligned} \frac{h_\tau(w; z)}{|t|^{5/2}} &= \frac{3}{16} w \left[ \left( 1 + \frac{7}{3\sqrt{3}} z \right) \right. \\ &\quad \left. - \frac{4}{3} \left( 1 + \frac{2}{\sqrt{3}} z \right) w^2 + \frac{16}{27} z |w|^3 \right] \\ &\quad + O(z w^5, z^2 w), \end{aligned} \quad (4.39)$$

$$\begin{aligned} \frac{h_{3\tau}(w; z)}{|t|^{3/2}} &= -\frac{1}{4} w \left[ \left( 1 + \frac{2}{\sqrt{3}} z \right) - \frac{4}{3} \left( 1 + \frac{2}{\sqrt{3}} z \right) w^2 \right. \\ &\quad \left. + \frac{4}{3} z |w|^3 \right] + O(z w^5, z^2 w). \end{aligned} \quad (4.40)$$

From this we see that, when  $z \neq 0$ , the triple surface at fixed  $t$  in the  $(g, h, h_3)$  space is no longer a straight

$$w_2(w, z) - w_{2,0\pm} = \mp \frac{1}{2} \sqrt{3} \left[ 1 + \frac{7z}{6\sqrt{3}} \right] w \mp \frac{1}{2\sqrt{3}} z w |w| - \frac{1}{2} w^2 - \frac{25}{18} z |w|^3 \pm \frac{1}{4} \sqrt{3} \left[ 1 + \frac{41z}{3\sqrt{3}} \right] w^3 + O(w^4, z^2 w), \quad (4.44)$$

$$w_3(w, z) - w_{3,0} = \left[ 1 + \frac{z}{4\sqrt{3}} \right] w^3 + O(w^4, z^2 w^3), \quad (4.45)$$

$$w_3(w, z) - w_{3,0\pm} = \pm \frac{1}{8} \sqrt{3} z |w| - \frac{9}{8} \left[ 1 + \frac{11z}{12\sqrt{3}} \right] w - \frac{3}{8} z w |w| \mp \frac{3\sqrt{3}}{16} \left[ 1 - \frac{19z}{12\sqrt{3}} \right] w^2 + O(w^3, z^2 w). \quad (4.46)$$

The main feature of these results is the nonanalyticity of the  $w_j(w)$  at  $O_+$  and  $O_-$ : in fact the edge of the three-phase monohedron has a *kink* at the points  $O_+$  and  $O_-$ , illustrated in Fig. 3 of Ref. 7, which may be contrasted with Fig. 4 below, which shows the classical view in the  $(w_1, w_2)$  plane. The kink may be exhibited explicitly by eliminating  $w$  between Eqs. (4.42) and (4.44) which yields

$$\begin{aligned} \Delta w_{2,\pm} &= w_2 - w_{2,0\pm} \\ &\approx \pm \sqrt{3} \Delta w_{1,0\pm} \left[ 1 \mp \frac{z}{\sqrt{3}} \operatorname{sgn}(\Delta w_{1,0\pm}) + \frac{z}{6\sqrt{3}} \right]. \end{aligned} \quad (4.47)$$

Evidently, the discontinuity in slope is proportional to  $z$ . It is clear from the explicit formulas that kinks

line in the plane  $h = -\frac{3}{4}|t|h_3$ ; instead, it is a twisted curve which is nonanalytic at  $w = 0$ .

From Eq. (A30) we find for  $z = 0$  but for all  $w$

$$w_\pm(w; 0) = -\frac{1}{2} w \pm \frac{1}{2} \sqrt{3} (1 - w^2)^{1/2}. \quad (4.41)$$

Using this and Eq. (4.27), the scaled density  $w_1$  at points near  $O_+$  and  $O_-$  conjugate to a point near  $O$  with  $w_1 \equiv w$  is

$$\begin{aligned} w_1(w; z) - w_{0\pm}(z) &= \pm \frac{z}{2\sqrt{3}} |w| - \frac{1}{2} \left[ 1 + \frac{z}{\sqrt{3}} \right] w \\ &\quad + \frac{1}{6} z w |w| \mp \frac{1}{4} \sqrt{3} \left[ 1 + \frac{z}{2\sqrt{3}} \right] w^2 \\ &\quad + O(w^3, z^2 w), \end{aligned} \quad (4.42)$$

where  $w_{0\pm}(z)$  follows from Eq. (4.37). The corresponding expressions for the  $w_2$  and  $w_3$  coordinates of the edge of the monohedron near  $O$  and near  $O_+$  and  $O_-$  follow from Eqs. (4.32) and (4.33). Recalling the values (4.36) and (4.37), the results may be written

$$w_2(w, z) - w_{2,0} = \left[ 1 + \frac{z}{\sqrt{3}} \right] w^2 + O(w^3, z^2 w^2), \quad (4.43)$$

also occur in the other two canonical projections, i.e., onto the  $(w_1, w_3)$  and  $(w_2, w_3)$  planes (see Figs. 5 and 6 below); however, even for large values of  $z$ , the kinks are not easily visible to the eye in these plots, so we do not reproduce them here.

The origin of the kinks at  $O_+$  and  $O_-$  is mathematically a consequence of the nonanalyticity of  $\zeta^{1/2}(M)$  as given by Eq. (4.17). This, in turn, is directly related to the vanishing of the inverse susceptibility  $1/\chi = \zeta$  (see I) in the ordered phase *on* (but not off) the symmetry plane. This feature is characteristic for systems with continuous  $O(n)$  symmetry. Thus we expect kinks in the edge of the monohedron to be present for all three-dimensional systems with  $n \geq 2$ . In normal fluid mixtures,<sup>6</sup> however, one has  $n = 1$ , and, although the edge might bend more or less sharply relative to classical theory, no kinks should appear at  $O_\pm$ .

It may be seen generally from Eq. (4.27) that the only nonanalytic points on the edge of the monohedron (at least to order  $z$ ) are  $O_+$  and  $O_-$ . However, the critical points,  $C_+$  and  $C_-$ , and the conjugate critical end-points,  $E_+$  and  $E_-$  (see Figs. 4–6, below, and Figs. 2 and 3 of Ref. 7), are also of particular interest and will be discussed next.

### C. Critical end-point region

The first task is to determine the precise location of the critical end-points on the edge of the three-phase monohedron in density space. At a critical end point,  $E$ , a noncritical phase of scaled density,  $w_E$ , coexists with a critical phase, or, equivalently, with two phases which have become identical at a critical point,  $C$ , with distinct density  $w_C$ . In terms of the scaled densities, the critical end-points are therefore parametrized by the values of  $w$ , say  $w_c(z)$ , which satisfy

$$w_+(w_c; z) = w_c \quad \text{or} \quad w_-(w_c; z) = w_c. \quad (4.48)$$

In the classical theory one finds simply  $w_c \equiv w_c(z=0) = \pm \frac{1}{2}$ . To solve Eq. (4.48) more generally, therefore, we expand the left-hand terms around  $w = \frac{1}{2}$  or  $w = -\frac{1}{2}$ . Owing to the symmetry, it suffices to consider only the (+) case. Then it is convenient to introduce a deviation variable,  $x$ , which measures the distance from the critical point  $C_+$  by setting

$$w_{+c}(z) = w_{+c}(0)(1+x) = \frac{1}{2}(1+x). \quad (4.49)$$

The expansion in powers of  $x$  is straightforward in principle but very tedious. Consider first Eq. (4.27) for  $m'_+(w)$ : for small  $x$  one finds

$$m'_+(w)/|t|^{1/2} = c_1(1 + \frac{1}{3}x + \frac{97}{315}x^2) + O(x^3), \quad (4.50)$$

where the numerical prefactor is

$$c_1 = \frac{245}{2 \times 3^6 \sqrt{3}} \approx 0.097017 \dots \quad (4.51)$$

Using Eq. (4.41) to compute the small  $x$  behavior of  $w_+(w)$  for  $z=0$  and combining the results yields

$$\begin{aligned} w_+(w; z) &= \frac{1}{2}[(1 + 2c_1z) - (1 - \frac{2}{3}c_1z)x \\ &\quad - \frac{1}{3}(1 - \frac{194}{105}c_1z)x^2] + O(x^3, zx, z^2). \end{aligned} \quad (4.52)$$

One can now rewrite the criticality relation (4.48) as

$$\begin{aligned} \frac{1}{2}(1+x_c) &= \frac{1}{2}[(1 + 2c_1z) - (1 - \frac{2}{3}c_1z)x_c] \\ &\quad + O(x_c^2, zx_c, z^2), \end{aligned} \quad (4.53)$$

which has the solution

$$x_c(z) = c_1z + O(z^2). \quad (4.54)$$

Thus the critical end-points are parametrized by

$$w_c(z) = \pm \frac{1}{2}(1 + c_1z) + O(z^2). \quad (4.55)$$

On using Eqs. (4.24)–(4.26) the critical end-point values of the fields are found to be

$$g_E(z) = \frac{3}{16}t^2 \left[ 1 - \frac{158}{3^5 \sqrt{3}}z \right] + O(z^2), \quad (4.56)$$

$$h_{E\pm}(z) = \mp \frac{1}{16}|t|^{5/2} \left[ 1 + \frac{407}{2 \times 3^4 \sqrt{3}}z \right] + O(z^2), \quad (4.57)$$

$$h_{3,E\pm}(z) = \pm \frac{1}{12}|t|^{3/2} \left[ 1 + \frac{349}{2 \times 3^4 \sqrt{3}}z \right] + O(z^2). \quad (4.58)$$

Note that by symmetry  $g$  takes the same value for  $E_+C_-$  and  $E_-C_+$ ; however,  $h$  and  $h_3$  are of opposite signs for the conjugate pair  $E_+C_-$  and  $E_-C_+$ , respectively. The critical points  $C_+$  and  $C_-$  in density space are similarly found to be

$$w_{C\pm}(z) = \pm \frac{1}{2}(1 + c_1z) + O(z^2), \quad (4.59)$$

$$w_{2,C\pm}(z) = \frac{1}{4} \left[ 1 - \frac{1213}{729 \sqrt{3}}z \right] + O(z^2), \quad (4.60)$$

$$w_{3,C\pm}(z) = \pm \frac{1}{8} \left[ 1 + \frac{733}{972 \sqrt{3}}z \right] + O(z^2), \quad (4.61)$$

while the densities of the conjugate end-points are

$$w_{E\pm}(z) = \pm \left[ 1 + \frac{211}{486 \sqrt{3}}z \right] + O(z^2), \quad (4.62)$$

$$w_{2,E\pm}(z) = 1 + \frac{601}{972 \sqrt{3}}z + O(z^2), \quad (4.63)$$

$$w_{3,E\pm}(z) = \pm \left[ 1 + \frac{341}{324 \sqrt{3}}z \right] + O(z^2). \quad (4.64)$$

It is also interesting to examine the behavior of the fields and densities in the neighborhood of the critical end-points, that is, for small values of

$$\Delta w = w - w_c(z), \quad (4.65)$$

at fixed (but small)  $z$ . To this end, one may expand Eqs. (4.7)–(4.9) in powers of  $x = 2w - 1$  and then combine terms in order to yield an expansion in powers of  $\Delta w$ . After tedious algebra, one obtains the expansions of the  $O(z)$  coefficients for the fields and densities which are presented in Table II. Finally, near the critical end-points the fields are found to

vary as

$$\frac{g - g_E}{t^2} = -\frac{2^5}{3^6\sqrt{3}} z \Delta w^2 - \frac{2^6}{3^7\sqrt{3}} z \Delta w^3 + O(z \Delta w^4, z^2) , \quad (4.66)$$

$$\frac{(h - h_{E+})}{|t|^{5/2}} = -\frac{3}{8} \left[ 1 + \frac{9631}{2 \times 3^7\sqrt{3}} z \right] \Delta w^2 - \frac{1}{4} \Delta w^3 + O(\Delta w^4, z \Delta w^3, z^2 \Delta w^2) , \quad (4.67)$$

$$\frac{(h_3 - h_{3,E+})}{|t|^{3/2}} = \frac{1}{2} \left[ 1 + \frac{2635}{2 \times 3^6\sqrt{3}} z \right] \Delta w^2 + \frac{1}{3} \Delta w^3 + O(\Delta w^4, z \Delta w^3, z^2 \Delta w^2) . \quad (4.68)$$

For the densities near the critical point  $C_+$ , one likewise finds

$$w_+ - w_{C+} = -\Delta w - \frac{2}{3} \Delta w^2 - \frac{4}{9} \Delta w^3 - \frac{16}{27} \Delta w^4 + O(\Delta w^5, z \Delta w^2) , \quad (4.69)$$

$$w_{2,+} - w_{2,C+} = - \left[ 1 + \frac{1703}{2 \times 3^6\sqrt{3}} z \right] \Delta w + \frac{1}{3} \Delta w^2 + \frac{8}{9} \Delta w^3 + O(\Delta w^4, z \Delta w^2, z^2 \Delta w) , \quad (4.70)$$

$$w_2 - w_{2,C+} = \left[ 1 + \frac{1703}{2 \times 3^6\sqrt{3}} z \right] \Delta w + \left[ 1 + \frac{1}{\sqrt{3}} z \right] \Delta w^2 + O(\Delta w^4, z^2 \Delta w) , \quad (4.71)$$

$$w_{3,+} - w_{3,C+} = -\frac{3}{4} \left[ 1 + \frac{1709}{4 \times 3^6\sqrt{3}} z \right] \Delta w + \Delta w^2 + O(\Delta w^3, z \Delta w^2) , \quad (4.72)$$

$$w_3 - w_{3,C+} = \frac{3}{4} \left[ 1 + \frac{1709}{4 \times 3^6\sqrt{3}} z \right] \Delta w + \frac{3}{2} \left[ 1 + \frac{1219}{4 \times 3^6\sqrt{3}} z \right] \Delta w^2 + O(\Delta w^3, z^2 \Delta w) . \quad (4.73)$$

The behavior near  $C_-$  follows by symmetry. Near the end-point  $E_-$  conjugate to  $C_+$  (see Figs. 4–6), one has

$$w_- - w_{E-} = \frac{2}{3} \left[ 1 + \frac{7645}{2 \times 3^7\sqrt{3}} z \right] \Delta w^2 + \frac{4}{9} \Delta w^3 + \frac{16}{27} \Delta w^4 + O(\Delta w^5, z \Delta w^3, z^2 \Delta w^2) , \quad (4.74)$$

$$w_{2,-} - w_{2,E-} = -\frac{4}{3} \left[ 1 + \frac{2585}{3^7\sqrt{3}} z \right] \Delta w^2 - \frac{8}{9} \Delta w^3 + O(\Delta w^4, z \Delta w^3, z^2 \Delta w^2) , \quad (4.75)$$

$$w_{3,-} - w_{3,E-} = 2 \left[ 1 + \frac{11951}{4 \times 3^7\sqrt{3}} z \right] \Delta w^2 + \frac{4}{3} \Delta w^3 + O(\Delta w^4, z \Delta w^3, z^2 \Delta w^2) . \quad (4.76)$$

TABLE II. Expansions of  $y' = g'$ ,  $h'$ ,  $h'_3$ , and  $m'_\pm$  for small  $\Delta w = w - w_c(z) = \frac{1}{2}x + O(z) = m/|t|^{1/2} - \frac{1}{2} + O(z)$ , as  $y' = y'_0(1 + a_1\Delta w + a_2\Delta w^2 + \dots)$ . Note also that for  $g'$  one has  $a_3 = 512/3^379$ .

$y'$	$y'_0$	$a_1$	$a_2$
$g'$	$\frac{79t^2}{2^33^4\sqrt{3}}$	0	$\frac{256}{3^279}$
$h'$	$\frac{407 t ^{5/2}}{2^53^4\sqrt{3}}$	$\frac{490}{3 \times 407}$	$-\frac{17792}{9 \times 407}$
$h'_3$	$\frac{349 t ^{3/2}}{2^33^5\sqrt{3}}$	$\frac{490}{3 \times 349}$	$-\frac{4780}{3 \times 349}$
$m'_+$	$\frac{245 t ^{1/2}}{2 \times 3^6\sqrt{3}}$	$\frac{2}{3}$	$\frac{388}{315}$
$m'_-$	$-\frac{211 t ^{1/2}}{2 \times 3^5\sqrt{3}}$	$\frac{490}{3^2211}$	$-\frac{13820}{3^2211}$

Near the critical end-points we thus confirm that the behavior is purely analytic. In other words, the edge of the three-phase monohedron near  $C_\pm$  and  $E_\pm$  has qualitatively the same properties as in classical theory. In particular, there is no flattening of the edge near the critical points  $C_+$  and  $C_-$ , as would be anticipated for systems with  $n < \infty$  on the basis of the nonclassical value of the inverse coexistence component ( $1/\beta > 2$ ) arising on the critical surface. Indeed, such flattening has been observed in experiments on real multicomponent fluids<sup>6</sup> where  $1/\beta \approx 2.9$ . Our present calculations, however, are restricted to  $n = \infty$  for which  $1/\beta = 2$  (see I), so that nonanalytic flattening should not be expected.

#### E. Characterization of nonclassical deviations

The quantitative deviations of the shape of the three-phase monohedron from the classical predictions are best expressed in terms of the dimension-

less ratios<sup>7</sup>

$$\mathcal{R}_{0,j} = [O_+O]_j/[E_+O]_j \quad (j=1,2,3), \quad (4.77)$$

and

$$\mathcal{R}_{c,j} = [C_+O]_j/[E_+O]_j \quad (j=1,2,3), \quad (4.78)$$

evaluated asymptotically as  $T \rightarrow T_t$ . Here  $[XY]_j$  denotes the projection of the line  $XY$  in density space (at fixed  $T$ ) onto the  $w_j$  axis. Thus the ratios specify the location of the critical points  $C_+$  and  $C_-$  and the points  $O_+$  and  $O_-$ , conjugate to the central point  $O$ , relative to the end points  $E_+$  and  $E_-$ . As demonstrated in the Appendix, the ratios take simple universal values in classical theory [see Eq. (A53)]. However, in the limit  $n \rightarrow \infty$  the ratios are nonuniversal and, to first order in  $z$ , may be written

$$\mathcal{R}_{0,j}(z) = (\frac{3}{4})^{j/2}(1 - e_{0,j}z), \quad (4.79)$$

$$\mathcal{R}_{c,j}(z) = (\frac{1}{2})^j(1 - e_{c,j}z). \quad (4.80)$$

The coefficients  $e_{0,j}$  and  $e_{c,j}$  may be computed from Eqs. (4.36) and (4.37), which specify the coordinates of  $O$ ,  $O_+$ , and  $O_-$ , and from Eqs. (4.59)–(4.64), which specify the points  $C_\pm$  and  $E_\pm$ . One finds

$$e_{0,1} = \frac{65}{3^5\sqrt{3}}, \quad e_{0,2} = \frac{17}{2 \times 3^5\sqrt{3}}, \quad e_{0,3} = \frac{49}{2 \times 3^4\sqrt{3}}, \quad (4.81)$$

and

$$e_{c,1} = \frac{194}{3^6\sqrt{3}}, \quad e_{c,2} = \frac{47}{2 \times 3^6\sqrt{3}}, \quad e_{c,3} = \frac{145}{2 \times 3^5\sqrt{3}}. \quad (4.82)$$

The corresponding numerical values are presented in Table III. Note that  $e_{0,j}$  differs from  $e_{c,j}$  by only a few percent (for  $j=1,2,3$ ).

Evidently, the nonclassical deviations are, at least to first order in  $z$ , comparatively small. In fact, currently available data for multicomponent fluids<sup>6</sup> are not sufficiently precise to observe deviations of this general magnitude. Nevertheless, if for fluids one finds  $z \approx 0.1$  to  $0.3$ , as suggested for magnets and  $^3\text{He}$ - $^4\text{He}$  mixtures,<sup>7</sup> the predicted deviations

TABLE III. Numerical values of monohedron nonclassical shape coefficients.

$j$	1	2	3
$e_{0,j}$	0.154 435	0.020 195	0.174 630
$e_{c,j}$	0.153 643	0.018 611	0.172 254

should be detectable. The ratios  $\mathcal{R}_{0,1}$  and  $\mathcal{R}_{c,1}$  are the most accessible to observation. Indeed, as  $|t| \rightarrow 0$  (or  $T \rightarrow T_t$ ), the projections  $[O_+O]_j$ ,  $[C_+O]_j$ , and  $[E_+O]_j$  vanish as  $|t|^{j/2}$  so that, for small enough  $|t|$ , one simply has

$$\begin{aligned} \mathcal{R}_{0,1}(z) &\approx (O_+O_-)/(E_+E_-), \\ \mathcal{R}_{c,1}(z) &\approx (C_+C_-)/(E_+E_-), \end{aligned} \quad (4.83)$$

where  $(XY)$  denotes the distances directly observed in density space. Thus, to measure the first pair of ratios, there is no need to determine the directions of the scaling axes  $w_1$ ,  $w_2$ , and  $w_3$  in the real, unscaled density (or concentration) space. This is a reflection of the fact<sup>6</sup> that the monohedron in density space collapses asymptotically to a line (along the  $w_1$  axis) when  $T \rightarrow T_t$ .

In classical theory, as demonstrated in the Appendix, the coexistence triangles are, asymptotically, all parallel to one another and to a plane containing the  $w_2$  axis. Moreover, the coexistence tie lines  $E_+C_-$  and  $E_-C_+$  are asymptotically tangent to the edge of the monohedron at  $C_-$  and  $C_+$ , respectively, when projected onto the  $(w_1, w_3)$  plane (see Fig. 5 below), and at  $E_+$  and  $E_-$ , respectively, when projected onto the  $(w_3, w_2)$  plane (see Fig. 6 below). We may also check these predictions for nonzero  $z$ .

Consider the tie line  $E_+C_-$ : from Eqs. (4.59)–(4.64) its slope in the  $(w_1, w_3)$  plane to order  $z$  is

$$\frac{w_{3,E+} - w_{3,C-}}{w_{E+} - w_{C-}} = \frac{3}{4} \left[ 1 + \frac{655}{4 \times 3^5\sqrt{3}} z \right], \quad (4.84)$$

where the coefficient of  $z$  has the value  $0.389 \dots$ . On the other hand, by Eq. (4.73) the slope of the tangent at  $C_-$  in the  $(w_1, w_3)$  plane to order  $z$  is

$$\left( \frac{dw_3}{dw} \right)_{C-} = \frac{3}{4} \left[ 1 + \frac{1709}{4 \times 3^6\sqrt{3}} z \right], \quad (4.85)$$

where the numerical value of the coefficients is  $0.338 \dots$ . Thus the tie line is no longer tangent at  $C_-$ , although the difference in slope is surprisingly small, indeed only about  $0.038z$ .

Likewise, in the  $(w_2, w_3)$  plane the slope of the tie line is

$$\frac{w_{3,E+} - w_{3,C-}}{w_{2,E+} - w_{2,C-}} = \frac{3}{2} \left[ 1 - \frac{1049}{4 \times 3^6\sqrt{3}} z \right], \quad (4.86)$$

while, for the tangent at  $E_+$ , the results (4.75) and (4.76) yield

$$\left( \frac{dw_3}{dw_2} \right)_{E+} = \frac{3}{2} \left[ 1 + \frac{179}{4 \times 3^5\sqrt{3}} z \right]. \quad (4.87)$$

The numerical values of the first-order coefficients are  $0.207 \dots$  and  $0.106 \dots$ , respectively, so that tangency is again destroyed for nonzero  $z$ , but still to only a small degree.

In order to check the coexistence triangles for parallelism, we compute the unit vector  $\bar{v} = (v_1, v_2, v_3)$  normal to a triangle in  $(w_1, w_2, w_3)$  space. If  $w_j$  and  $w_{j\pm}$  ( $j = 1, 2, 3$ ) denote the coordinates of the three vertices of a coexistence triangle, the direction cosines are given by

$$v_i = D_i / \left[ \sum_{j=1}^3 D_j^2 \right]^{1/2} \quad (i = 1, 2, 3), \quad (4.88)$$

where, with  $(i, j, k)$  an even permutation of  $(1, 2, 3)$ ,

$$D_i = \begin{vmatrix} w_{j+} - w_j & w_{k+} - w_k \\ w_{j-} - w_j & w_{k-} - w_k \end{vmatrix}. \quad (4.89)$$

For the central, symmetric triangle  $O_+OO_-$  one finds from Eqs. (4.36) and (4.37) the values

$$\begin{aligned} v_{1,O} &= -\frac{3}{5} \left[ 1 + \frac{28}{75\sqrt{3}} z \right], \quad v_{2,O} = 0, \\ v_{3,O} &= \frac{4}{5} \left[ 1 - \frac{21}{100\sqrt{3}} z \right], \end{aligned} \quad (4.90)$$

to first order in  $z$ . Thus, as in classical theory the central triangle always lies in a plane containing the  $w_2$  axis (see Fig. 5 below); however, the slope of  $O_+O_-$  in the  $(w_1, w_3)$  plane varies slightly with  $z$ .

Near the critical end-points one can use Eqs. (4.69)–(4.76) to compute  $\bar{v}$  for small  $\Delta w = w - w_c$  and then calculate the limit  $\Delta w \rightarrow 0$ . The limiting slope of the coexistence triangles as they degenerate into the end-point tie line is thence found to be

$$\begin{aligned} v_{1,E} &= -\frac{3}{5} \left[ 1 + \frac{22556}{3^7 5^2 \sqrt{3}} z \right], \quad v_{2,E} = \frac{2^7}{3^6 5 \sqrt{3}} z, \\ v_{3,E} &= \frac{4}{5} \left[ 1 - \frac{5639}{4 \times 3^5 5^2 \sqrt{3}} z \right], \end{aligned} \quad (4.91)$$

correct to order  $z$ . By comparison with Eq. (4.90) we see that the coexistence triangles are *not parallel* for  $z > 0$ . However, the angles between the triangles are extremely small. Indeed, if  $\alpha_{OE}$  is the angle between the normals to the central and limiting coexistence triangles one has

$$\alpha_{OE} = \frac{8\sqrt{10889}}{3^6 25 \sqrt{3}} z \approx (1.5152)^\circ z, \quad (4.92)$$

where the right-hand expression is in degrees of arc. Thus, within the validity of the first-order expansion in  $z$ , the angles predicted are less than  $1^\circ$ . It seems unlikely that such small angular deviations could be reliably detected, especially when it is remembered that  $\alpha_{OE}$  has been defined within the *scaled* density space  $(w_1, w_2, w_3)$  rather than within the space of real densities  $(m_1, m_2, m_3)$ .

## V. CONCLUDING COMMENTS

In the foregoing we have analyzed in detail the tricritical equation of state for the basic spin model with  $n$ -component spins  $\vec{S}_j$  [see the Hamiltonian displayed in (2.1)], in the exactly soluble, infinite-component limit,  $n \rightarrow \infty$ , in  $d = 3$  spatial dimensions. In particular, we have discussed the phase diagrams in field space and in density space, where the three-phase monohedron resides, for temperatures below tricriticality. The results, even in the asymptotic scaling region, are nonuniversal but are parametrized by a single marginal variable,  $z = c_0(a/R_0)^d$ , where  $R_0$  is the range of the basic spin-spin coupling [see Eq. (2.10)] and, here,  $d = 3$ . In the plane of symmetry (where the odd fields  $h$  and  $h_3$ , coupling to  $s$  and  $s^3$ , vanish) explicit results were obtained for general  $z$  in the range  $(0, 1)$  [see Eqs. (3.36), (3.41), (3.43), and (3.45)]: Note that at  $z = 1$  a new sort of multicritical point appears: for  $z > 1$  the tricritical point is replaced by a critical end-point (see I). However, off the plane of symmetry, as needed to study the three-phase monohedron, algebraic complications preclude an explicit evaluation of the deviations from classical theory: instead, various amplitude ratios, etc. [see Eqs. (4.77)–(4.82), (4.84)–(4.87), and (4.92)] have been evaluated to first order in  $z$ . [Recall that the zeroth-order ( $z = 0$ ) results are identical with classical theory, which is presented systematically in the Appendix.]

Real magnetic and fluid systems<sup>4–6</sup> should be described not by  $n = \infty$  but rather by  $n = 1$  or 2. Nevertheless, as shown in Ref. 7, the nonuniversal amplitude ratios calculated for  $n = \infty$  give a surprisingly consistent description of deviations from classical theory observed in the best current experiments.<sup>4–6</sup> These experiments can be well fitted by pure power laws with the classical tricritical exponents. None of the data seem to require the logarithmic correction factors which are predicted for finite  $n$  on the basis of the renormalization-group calculations.<sup>1,3</sup> Although the current renormalization-group theories<sup>3,19</sup> do not yield a complete equation of state (in particular, they fail to describe the critical surface properly), there seems no good reason to doubt that the predicted logarithmic factors should be present in the full solution of the basic model for finite  $n$ , and, presumably, have some role to play in the description of experimental results. In Ref. 7 it was suggested that this paradox might find its resolution in the replacement of the fixed, nonuniversal parameter  $z$  for  $n = \infty$ , by a slowly varying logarithmic function,  $\tilde{z}$ , of  $t$  and the other fields, when  $n < \infty$ . This suggestion can be made more concrete by reference to the renormalization-group calculations of Stephen, Abraham, and Straley.<sup>3</sup>

As is customary,<sup>20</sup> the calculation of Stephen *et al.* starts from a field-theoretic formulation of the origi-

nal spin Hamiltonian in the form

$$\frac{\mathcal{H}}{k_B T} = \int d^d x \left( \frac{1}{2} r_0 |\vec{s}(x)|^2 + \frac{1}{2} |\nabla \vec{s}|^2 + \frac{u_4}{4!} |\vec{s}(x)|^4 + \frac{u_6}{6!} |\vec{s}(x)|^6 \right). \quad (5.1)$$

If, following standard procedures (involving the Fourier representation, etc.),<sup>20</sup> one converts Hamiltonian (2.1) to this form, one discovers, in particular, the identification

$$u_6 = 5! b_\phi k_B^2 T^2 V a^{2d} / J_0^2 n^2 R_0^6 \propto V z^2 / n^2, \quad (5.2)$$

for  $d=3$  [where  $b_\phi=1$  if the spin-spin interaction shape function,  $\varphi(x)$ , is scaled appropriately while  $R_0$  is defined as a suitably normalized second moment of  $J(R)$ ]. Now Stephen *et al.*<sup>3</sup> argue that, away from the critical surfaces, the equation of state can be calculated to leading logarithmic order by perturbation theory with the replacement of  $u_6$  by a renormalized sixth-order coupling constant

$$\Gamma_6 = \frac{u_6}{L(r)}, \quad L(r) = 1 + \frac{3n+22}{480\pi^2} u_6 \ln r^{-1}, \quad (5.3)$$

where  $r$  is essentially the inverse susceptibility  $1/\chi$  (although this identification has serious difficulties for  $n \geq 2$  in the ordered region on the symmetry plane, since  $1/\chi$  vanishes identically for  $d < 4$  due to long-wavelength, Goldstone-type fluctuations). Comparison with Eq. (5.2) then suggests that  $z$  should, equivalently, be replaced by a renormalized value

$$\tilde{z} \equiv z_R = \frac{z}{[1 + (c_1 z^2/n) \ln r^{-1}]^{1/2}}, \quad (5.4)$$

with  $c_1 = [3 + (22/n)] b_\phi k_B^2 T^2 V / 4\pi^2 J_0^2 c_0^2$ . The inverse susceptibility scales like  $t^2$ , so the renormalized  $z$  parameter vanishes as  $1/(\ln|t|^{-1})^{1/2}$  when the tricritical point is approached: various critical amplitude ratios should then asymptotically achieve their classical values. However,  $(\ln|t|^{-1})^{-1/2}$  is a very slow decay, so that in practical experiments one may expect to see an effectively constant value of  $z_R$  over several decades of  $t$  and nonclassical, nonuniversal amplitude ratios. This could account for the observed success of the fixed- $z$  ( $n=\infty$ ) formulation in describing the experiments. Note also that when  $n \rightarrow \infty$  the renormalized parameter reduces simply to  $z$ .

A full substantiation of the concept of a thermodynamically varying renormalized value of  $z$  for finite  $n$  will have to await further, more extensive calculations. In particular, it remains important to achieve a description of the critical surfaces for  $n < \infty$  in which the correct, nonclassical exponents,  $\beta$ ,  $\gamma$ , etc. are properly embodied. As mentioned in Sec. IV D, this seems crucial for a satisfactory account of the shape of the three-phase monohedron near the critical points  $C_+$  and  $C_-$ .

## ACKNOWLEDGMENTS

This work has enjoyed the support of the National Science Foundation, in part through the Materials Science Center at Cornell University, of the Swiss National Science Foundation, through the award of a fellowship to S.S., and of the John Simon Guggenheim Memorial Foundation, through the award of a fellowship to M.E.F. We are also grateful to Professor B. I. Halperin, Professor Michael J. Stephen, and Dr. Jeffrey R. Fox for conversations and comments.

## APPENDIX A: COEXISTENCE OF TRICRITICAL PHASES IN CLASSICAL THEORY

In this appendix we present an exposition of the classical or Landau phenomenological theory of the coexistence of phases in the tricritical region. As mentioned, this analysis is not entirely obvious, and does not seem to be in the literature. Furthermore, we need it here since the classical theory becomes valid in the long range or van der Waals limit ( $\dot{p} = z = 0$ ) and provides a basis for our perturbation expansion in  $z$ .

According to the classical theory the free energy may be written

$$F(t, g, h, h_3) = F_0(t, g, h, h_3) + \min_m [\Phi(m; t, g, h, h_3)], \quad (A1)$$

where  $F_0(t, g, h, h_3)$  is regular in the four fields  $t, g, h$ , and  $h_3$ , while, in the tricritical region,  $\Phi$  is a polynomial of sixth degree in  $m$ , the order parameter, namely,

$$\Phi(m; t, g, h, h_3) = -hm + \frac{1}{2} g m^2 - h_3 m^3 + \frac{1}{4} t m^4 + \frac{1}{6} m^6. \quad (A2)$$

Note that this polynomial is, in fact, the most general sixth-order polynomial for this purpose, since a term in  $m^5$  could be eliminated by replacing  $m$  by  $m + m_0$ , choosing  $m_0$  appropriately, and redefining the four fields by corresponding shifts. Likewise, any constant term, independent of  $m$ , can be absorbed in  $F_0$ .

In the case of the spherical model limit the constraint equation (2.8) or (2.16) reduces to  $\tilde{m} = m^2$  when  $\dot{p}$  or  $z$  approach zero, and the free energy then reduces to the form (A1). To analyze the phase diagram, which is determined by the possible states of coexisting phases, we exploit the fact that  $\Phi(m)$  is an algebraic polynomial and hence can be factored uniquely in terms of its roots.<sup>21</sup>

### 1. Coexistence manifold

There will be coexistence of two phases with order parameter  $m_+$  and  $m_- < m_+$  in the system defined by Eqs. (A1) and (A2) if  $\Phi(m)$  has two equal minima.



In this case  $\Phi(m)$  can be written

$$\Phi(m) = \frac{1}{6}(m - m_+)^2(m - m_-)^2(m^2 - 2am + b) + \Phi_0, \quad (\text{A3})$$

with the condition

$$b \geq a^2, \quad (\text{A4})$$

which is necessary and sufficient to prevent the existence of a third minimum with a lower value of  $\Phi$ ; at  $b = a^2$  a third *equal* minimum arises. Note that  $\Phi_0$  is just a constant. Now, by expanding Eq. (A3) and comparing with Eq. (A2) one obtains the relations between the fields  $t, g, h, h_3$  and  $m_+, m_-, a, b$ , and  $\Phi_0$ , namely,

$$m_+ + m_- + a = 0, \quad (\text{A5})$$

$$t = \frac{2}{3}[(m_+ + m_-)^2 + 2m_+m_- + 4a(m_+ + m_-) + b], \quad (\text{A6})$$

$$h_3 = \frac{1}{3}[m_+m_-(m_+ + m_-) + a(m_+ + m_-)^2 + 2am_+m_- + b(m_+ + m_-)], \quad (\text{A7})$$

$$g = \frac{1}{3}[m_+^2m_-^2 + 4am_+m_-(m_+ + m_-) + b(m_+ + m_-)^2 + 2bm_+m_-], \quad (\text{A8})$$

$$h = \frac{1}{3}m_+m_-[am_+m_- + b(m_+ + m_-)], \quad (\text{A9})$$

$$\Phi_0 = -\frac{1}{6}bm_+^2m_-^2. \quad (\text{A10})$$

If, say, Eq. (A5) is used to eliminate  $m_-$ , the Eqs. (A6) to (A9) may be regarded as providing a parametric representation, in terms of  $(m_+, a, b)$ , of the two-phase coexistence manifold in the thermodynamic field space  $(t, g, h, h_3)$ . Evidently the two-phase coexistence manifold has dimension 3, and, hence, codimension 1. It is convenient and somewhat more explicit to reexpress this situation by using Eqs. (A5), (A6), and (A7) to eliminate  $m_+, m_-$ , and  $b$  in favor of  $a, t$ , and  $h_3$ . This yields

$$g = \frac{1}{4}(t^2 + 2ta^2 + \frac{20}{9}a^4) - \frac{4}{3}h_3(a + \frac{3}{4}a^{-2}h_3), \quad (\text{A11})$$

$$h = -\frac{1}{6}a^3(t + \frac{4}{3}a^2) + \frac{1}{2}h_3(t + \frac{2}{3}a^2 + 2a^{-1}h_3), \quad (\text{A12})$$

$$m_{\pm} = -\frac{1}{2}a \pm (-\frac{1}{2}t - \frac{5}{12}a^2 - a^{-1}h_3)^{1/2}. \quad (\text{A13})$$

Of course the coexistence minima are real only if

$$t \leq -\frac{5}{6}a^2 - 2a^{-1}h_3. \quad (\text{A14})$$

Moreover, the condition (A4) can now be rewritten

$$h_3/a \leq \frac{1}{3}a^2 + \frac{1}{4}t. \quad (\text{A15})$$

The coexistence manifold is therefore described by Eqs. (A11) and (A12) provided that both conditions (A14) and (A15) are satisfied.

## 2. Critical surfaces

The coexistence manifold is bounded by critical surfaces of dimension 2 and codimension 2 in the space  $(t, g, h, h_3)$ . On a critical surface one must have  $m_+ = m_-$  which implies that Eq. (A14) is satisfied as an equality so that

$$a^3 + \frac{6}{5}ta_c + \frac{12}{5}h_3 = 0. \quad (\text{A16})$$

On using this to eliminate  $t$  in Eq. (A15) we obtain

$$12h_3/a_c \leq a_c^2. \quad (\text{A17})$$

A solution of Eq. (A16) satisfying this condition will, on introduction in Eqs. (A11) and (A12), determine a critical surface  $g_c(t, h_3)$ ,  $h_c(t, h_3)$ . One may, alternatively, use Eq. (A16) to eliminate  $t$  in Eqs. (A11) and (A12) and thence obtain the critical surface parametrized by  $a$  and  $h_3$ ; this gives

$$g_c = \frac{5}{16}a^2(a^2 - \frac{24}{5}a^{-1}h_3), \quad (\text{A18})$$

$$h_c = -\frac{1}{12}a^3(a^2 - 3a^{-1}h_3), \quad (\text{A19})$$

$$t_c = -\frac{5}{6}(a^2 + \frac{12}{5}a^{-1}h_3), \quad (\text{A20})$$

$$m_c = -\frac{1}{2}a. \quad (\text{A21})$$

If  $h_3 = 0$  and  $t < 0$  these equations reduce to

$$g_c = \frac{5}{16}a^4, \quad h_c = -\frac{1}{12}a^5, \quad t_c = -\frac{5}{6}a^2. \quad (\text{A22})$$

Finally, then the *critical lines* bounding the symmetrically disposed tricritical "wings" (for  $h_3 = 0$ ) are given by

$$g_c(t) = \frac{9}{20}t^2, \quad h_c(t) = \pm \frac{\sqrt{2}}{3}(\frac{3}{5})^{5/2}|t|^{5/2}, \quad (\text{A23})$$

and

$$m_c(t) = \pm (\frac{3}{10})^{1/2}|t|^{1/2}. \quad (\text{A24})$$

For  $h_3 = 0$  and  $t \geq 0$  one obtains the *lambda line* given simply by

$$g_c = h_c = m_c = 0 \quad (\text{all } t \geq 0). \quad (\text{A25})$$

An alternative, rather more explicit representation of the critical surface may be obtained by using Eq. (A13) to conclude  $a = -2m_c$ , as in Eq. (A21). Then one may eliminate  $h_3$  between Eqs. (A16) and (A18) to obtain

$$15m_c^4 + 3tm_c^2 - g = 0. \quad (\text{A26})$$

This is simply a quadratic equation for  $m_c^2$  and hence may be solved explicitly to yield  $m_c(t, g)$ . (One must, of course, choose the root which gives  $m_c^2 \geq 0$ .) Then by solving Eq. (A16) for  $h_{3c}$  and substituting in

Eq. (A19) one obtains

$$\begin{aligned} h_c(t, g) &= \frac{1}{5} m_c (2g - t m_c^2) , \\ h_{3c}(t, g) &= m_c (t + \frac{10}{3} m_c^2) , \end{aligned} \quad (\text{A27})$$

so that for given  $t$  and  $g$  the coexistence surface may be exhibited in closed form.

### 3. Triple surface

When Eq. (A4) or, equivalently, (A15) is satisfied as an equality, the polynomial  $\Phi(m)$  in Eq. (A3) has three equal minima and can be rewritten<sup>21</sup>

$$\Phi(m) = \frac{1}{6} (m - m_+)^2 (m - m_-)^2 (m - m_0)^2 + \Phi_0 . \quad (\text{A28})$$

In this case *three* phases coexist: Thus with  $a \equiv m_0$  the condition

$$b - a^2 \equiv b - m_0^2 = \frac{8}{3} m_0^{-1} (m_0^3 + \frac{3}{4} t m_0 - 3 h_3) = 0 , \quad (\text{A29})$$

determines the *triple surface*. Using this to eliminate  $h_3$  in (A13) one obtains, for  $t < 0$ , the three values

$$m_{\tau \pm} = \frac{1}{2} [-m_0 \pm \sqrt{3} (|t| - m_0^2)^{1/2}] , \quad (\text{A30})$$

$$m_{\tau} = m_0 . \quad (\text{A31})$$

The triple surface exists, of course, only for  $t < 0$  and  $m_0$  ranges only from  $-|t|^{1/2}$  to  $+|t|^{1/2}$ . From Eq. (A29) one finds the value of  $h_3$  on the triple surface as

$$h_{3, \tau} = \frac{1}{3} m_0 (m_0^2 - \frac{3}{4} |t|) \quad (t < 0) . \quad (\text{A32})$$

Introducing this value in Eqs. (A11) and (A12) finally yields

$$g_{\tau} = \frac{3}{16} t^2 , \quad (\text{A33})$$

$$h_{\tau} = -\frac{1}{4} |t| m_0 (m_0^2 - \frac{3}{4} |t|) \quad (t < 0) . \quad (\text{A34})$$

A  $(g, h)$  section of the phase diagram in field space is shown in Fig. 2. The triple surface appears as a straight line as follows from Eq. (A33).

### 4. Critical end-points and tricritical points

At a critical end-point two of the three coexisting phases become identical and, hence, critical. Inspection of Eq. (A30) shows that this happens only when the noncritical phase is given by

$$m_{\tau} = m_{E \pm} = \pm |t|^{1/2} , \quad (\text{A35})$$

corresponding to  $m_0 = \pm |t|^{1/2}$ . The conjugate critical end-point phases are thus specified by

$$m_{\tau c \pm} = \mp \frac{1}{2} |t|^{1/2} , \quad (\text{A36})$$

and, from Eqs. (A32) to (A34), the corresponding end-point fields are

$$g_{\tau c} = g_E = \frac{3}{16} t^2 , \quad (\text{A37})$$

$$h_{\tau c \pm} = h_{E \pm} = \mp \frac{1}{16} |t|^{5/2} , \quad (\text{A38})$$

$$h_{3, \tau c \pm} = h_{3, E \pm} = \pm \frac{1}{12} |t|^{3/2} . \quad (\text{A39})$$

Finally, the tricritical point is attained when all three

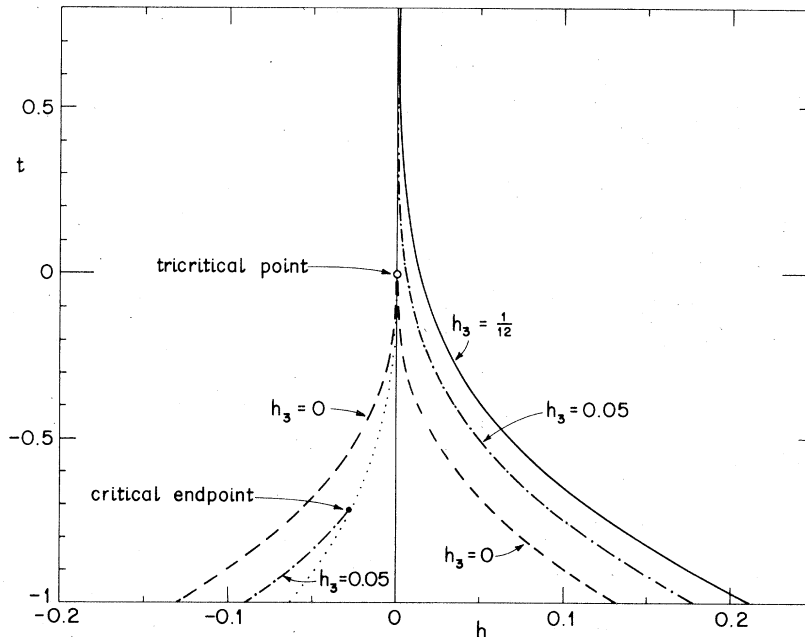


FIG. 3. Projections for the classical phase diagram of a critical end-point locus onto the  $(t, h)$  plane (dotted curve) and of the critical lines for  $h_3=0$  (dashed),  $0.05$  (dot-dash), and  $\frac{1}{12}$  (solid).

coexisting phases become identical which occurs only when

$$m_{\pm} = m_0 = 0, \quad t = g = h = h_3 = 0. \quad (\text{A40})$$

Figure 3 shows the projection of a critical end-point locus (dotted line) and of the critical lines onto the  $(t, h)$  plane for fixed values of  $h_3$  according to the above results.

### 5. Three-phase monohedron

Consider now the phase diagram at fixed  $t < 0$ , in the region where three phases coexist, in terms of the three densities

$$m_j = -\frac{\partial F}{\partial h_j} \quad (j = 1, 2, 3), \quad (\text{A41})$$

where we have written  $g \equiv -2h_2$  for convenience. From Eqs. (A1) and (A2) one sees that these densities always obey the simple relationship

$$m_2 = m_1^2, \quad m_3 = m_1^3, \quad (\text{A42})$$

provided one neglects the dependence of the regular term  $F_0$  on the  $h_j$ . This amounts to making appropriate subtractions of regular terms in the definition of the  $m_j$ . Note, however, that these terms are significant in the interpretation of experiments on fluid systems.<sup>18</sup> It is also convenient to introduce the scaling densities

$$w_j = m_j/|t|^{j/2} \quad (j = 1, 2, 3), \quad (\text{A43})$$

together with the scaling fields

$$x = g/t^2, \quad y = h/|t|^{5/2}, \quad y_3 = h_3/|t|^{3/2}. \quad (\text{A44})$$

If, furthermore, one sets  $m_0 = \sin\phi$  in Eqs. (A30) to (A34), the three-phase region is given by

$$w_1 = \sin\phi, \quad w_{1\pm} = -\sin(\phi \pm \frac{1}{3}\pi), \quad (\text{A45})$$

and, using Eq. (A42), one has

$$w_2 = \sin^2\phi = \frac{1}{2} - \frac{1}{2}\cos 2\phi, \quad (\text{A46})$$

$$w_{2\pm} = \frac{1}{2} + \frac{1}{2}\cos(2\phi \pm \frac{1}{3}\pi),$$

$$w_3 = \sin^3\phi = \frac{3}{4}\sin\phi - \frac{1}{4}\sin 3\phi, \quad (\text{A47})$$

$$w_{3\pm} = \pm \frac{3}{4}\cos(\phi \pm \frac{1}{6}\pi) \pm \frac{1}{4}\cos(3\phi \pm \frac{1}{2}\pi).$$

Finally, the values of the fields  $g$ ,  $h$ , and  $h_3$  in scaling form are simply

$$x = \frac{3}{16}, \quad y = \frac{1}{16}\sin 3\phi, \quad y_3 = -\frac{1}{12}\sin 3\phi. \quad (\text{A48})$$

When  $\phi = \pm \frac{1}{6}\pi$ , the  $w_j$ ,  $y$ , and  $y_3$  take their critical end-point values [see Eqs. (A35)–(A39)]. Therefore, at fixed  $t < 0$  the whole three-phase region is parametrized by

$$-\frac{1}{6}\pi \leq \phi \leq \frac{1}{6}\pi, \quad (\text{A49})$$

each value of  $\phi$  in this interval specifying three points in  $(w_1, w_2, w_3)$  space corresponding to three coexisting phases determining a coexistence triangle. As  $\phi$  varies, the vertices of the triangle move along a

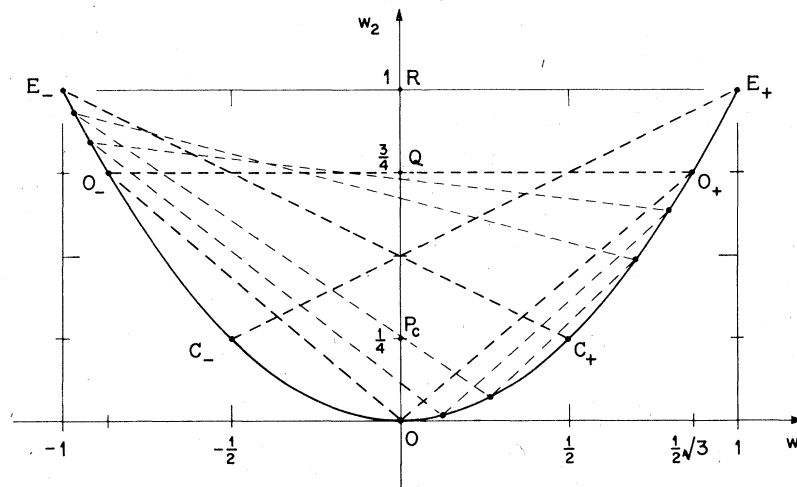


FIG. 4. Projection of the classical three-phase monohedron onto the  $(w_1, w_2)$  scaling variable plane showing various coexistence triangles (dashed lines), including the "central" or symmetric triangle  $O_+O_-$ , and the conjugate pairs of critical end-points  $C_+, E_-$ , and  $C_-, E_+$  joined by degenerate triangles, i.e., tie lines. The points  $P_c$ ,  $Q$ , and  $R$  lie on the  $w_2$  axis at the mid-points of the lines  $C_+C_-$ ,  $O_+O_-$ , and  $E_+E_-$ , respectively, in the full  $(w_1, w_2, w_3)$  space.

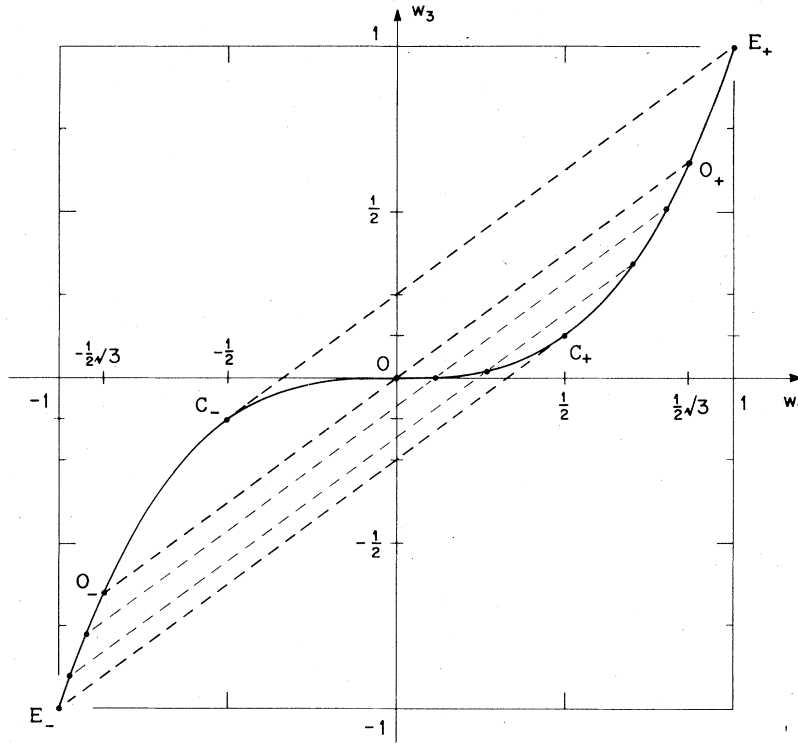


FIG. 5. Projection of the classical three-phase monohedron onto the  $(w_1, w_3)$  plane. Compare with Fig. 4: the same coexistence triangles are shown, but they appear as parallel straight lines in this view. Note the tangency at  $C_+$  and  $C_-$  of the end-point tie lines.

smooth, analytic curve given by [see Eq. (A42)]

$$w_2 = w_1^2, \quad w_3 = w_1^3, \quad (\text{A50})$$

with  $-1 \leq w_1 \leq 1$ . Different values of  $\phi$  in the interval (A49) specify distinct triangles which as  $\phi \rightarrow \pm \frac{1}{6}\pi$  degenerate into the critical end-point tie lines  $E_+C_-$  and  $E_-C_+$ . The coexistence triangles fill out a volume in density space which is bounded by a single ruled surface with a single smooth edge [given by Eq. (A50)]. The whole figure may thus be called the *three-phase monohedron*.

A general view of the monohedron is shown, for example, in Fig. 2 of Ref. 7. In Figs. 4–6 are drawn three canonical projections onto the  $(w_1, w_2)$  plane (parabolic), the  $(w_1, w_3)$  plane (cubic), and onto the  $(w_2, w_3)$  plane (cuspidal). In these figures the end-point  $E_+$  corresponds to  $\phi = +\frac{1}{6}\pi$  and is conjugate to the critical end-point  $C_-$ , whereas  $E_-$  and  $C_+$  correspond to  $\phi = -\frac{1}{6}\pi$ . The "central triangle",  $O_+OO_-$ , corresponds to  $\phi = 0$ , which represents the symmetry plane  $h = h_3 = 0$  in field space.

As pointed out in Ref. 7, the shape of the monohedron may be characterized in terms of the ratios

$$\alpha_{0,j} = [O_+O]_j / [E_+O]_j, \quad (\text{A51})$$

$$\alpha_{c,j} = [C_+O]_j / [E_+O]_j, \quad (\text{A52})$$

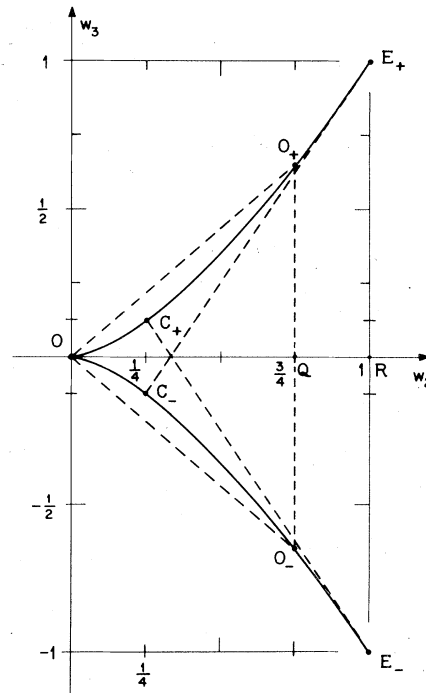


FIG. 6. Projection of the classical three-phase monohedron onto the  $(w_2, w_3)$  plane. Compare with Figs. 4 and 5: note the tangency of the endpoint tie lines at  $E_+$  and  $E_-$ .

for  $j = 1, 2, 3$ , where  $[XY]_j$  denotes the projection of the line  $XY$  onto the  $w_j$  axis. These ratios may be evaluated immediately from Eqs. (A45) to (A47) with the simple result

$$\alpha_{0,j} = (\frac{3}{2})^{j/2}, \quad \alpha_{c,j} = (\frac{1}{2})^j. \quad (\text{A53})$$

Finally, on using again Eqs. (A45)–(A47) it is easy to prove the following properties:

- (i) The coexistence triangles are parallel to one

another and lie in planes parallel to the  $w_2$  axis (see Fig. 5).

(ii) The tie line  $E_+C_-$  (or  $E_-C_+$ ) is tangent to the curve  $E_+O_+C_+OC_-O_-E_-$  at  $C_-$  (or  $C_+$ ) in the projection along the  $w_2$  axis (Fig. 5), and at  $E_+$  (or  $E_-$ ) in the projection along the  $w_1$  axis (Fig. 6).

As shown in Sec. IV, these metrical properties and the simple expressions (A50) and (A53) do not apply to the spherical model for  $\dot{p}, z > 0$ , although all the topological features of the monohedron survive.

<sup>1</sup>E. K. Riedel and F. J. Wegner, Phys. Rev. Lett. **29**, 349 (1972); F. J. Wegner and E. K. Riedel, Phys. Rev. B **7**, 278 (1973).

<sup>2</sup>R. B. Griffiths, J. Chem. Phys. **60**, 195 (1974).

<sup>3</sup>M. J. Stephen, E. Abrahams, and J. P. Straley, Phys. Rev. B **12**, 256 (1975); M. J. Stephen, Phys. Rev. B **12**, 1015 (1975).

<sup>4</sup>(a) G. Goellner, R. Behringer, and H. Meyer, J. Low Temp. Phys. **13**, 113 (1973); (b) E. K. Riedel, H. Meyer, and R. P. Behringer, *ibid.* **22**, 369 (1976); (c) D. R. Watts and W. W. Webb, in *Low Temperature Physics, LT-13*, edited by W. J. O'Sullivan *et al.* (Plenum, New York, 1974), Vol. 1, p. 581.

<sup>5</sup>(a) J. A. Griffin and S. E. Schnatterly, Phys. Rev. Lett. **33**, 1576 (1974); (b) N. Giordano and W. P. Wolf, Phys. Rev. Lett. **35**, 799 (1975); (c) N. J. Giordano, Ph. D. thesis, (Yale University, 1977) (unpublished).

<sup>6</sup>J. C. Lang, Jr., and B. Widom, Physica (Utrecht) A **81**, 190 (1975).

<sup>7</sup>M. E. Fisher and S. Sarbach, Phys. Rev. Lett. **41**, 1127 (1978).

<sup>8</sup>S. Sarbach and M. E. Fisher, Phys. Rev. B **18**, 2350 (1978); this paper will be denoted I. See also S. Sarbach and M. E. Fisher, J. Appl. Phys. **49**, 1350 (1978).

<sup>9</sup>V. J. Emery, Phys. Rev. B **11**, 239 (1975); **11**, 3397 (1975).

<sup>10</sup>S. Sarbach and T. Schneider, Phys. Rev. B **16**, 347 (1977).

<sup>11</sup>See, e.g., J. M. Kincaid and E. G. D. Cohen, Phys. Rep. **22**, 57 (1975).

<sup>12</sup>E. K. Riedel, Phys. Rev. Lett. **28**, 675 (1972).

<sup>13</sup>A. Hankey, H. E. Stanley, and T. S. Chang, Phys. Rev. Lett. **29**, 278 (1972).

<sup>14</sup>M. E. Fisher, in *Magnetism and Magnetic Materials – 1974*, edited by C. D. Graham, Jr., G. H. Lander, and J. J. Rhyne, AIP Conf. Proc. No. 24 (AIP, New York, 1975), p. 273; M. E. Fisher and D. Jasnow, *Theory of Correlations in the Critical Region* (Academic, New York, to be published), Appendix A.

<sup>15</sup>D. H. Saul, M. Wortis, and D. Stauffer, Phys. Rev. B **9**, 4964 (1974).

<sup>16</sup>D. P. Landau, Phys. Rev. Lett. **28**, 449 (1972); B. L. Arora and D. P. Landau, in *Magnetism and Magnetic Material – 1972*, edited by C. D. Graham, Jr. and J. J. Rhyne, AIP Conf. Proc. No. 10 (AIP, New York, 1973), p. 870.

<sup>17</sup>M. Blume, V. J. Emery, and R. B. Griffiths, Phys. Rev. A **4**, 1071 (1971).

<sup>18</sup>J. R. Fox, J. Chem. Phys. **69**, 2231 (1978).

<sup>19</sup>I. D. Lawrie, J. Phys. A **12**, 919 (1979).

<sup>20</sup>See, e.g., M. E. Fisher, Rev. Mod. Phys. **46**, 597 (1974).

<sup>21</sup>We are indebted to Dr. J. R. Fox and Professor R. B. Griffiths for this method of approach.